La borsa di dottorato è stata cofinanziata con risorse del
Programma Operativo Nazionale Ricerca e Innovazione 2014-202 (CCI 2014IT16M2OP005)
Fondo Sociale Europeo, Azione I.1 "Dottorati Innovativi con caratterizzazione Industriale"

UNIVERSITA' DELLA CALABRIA

Dipartimento di Biologia, Ecologia e Scienze della Terra

Dottorato di Ricerca in

Life Science and Technology

Con il contributo di

Pon R&I 2014-2020

CICLO

XXXVI

RHEOLOGICAL STUDY OF BITUMINOUS ECOBASES FOR COLD RECYCLING

Settore Scientifico Disciplinare: ING-IND/24

Coordinatore: Ch.mo Prof. Tommaso Angelone

Firma _____ Tommaso Angelone 25.06.2024 10:33:44 GMT+01:00

Supervisore: Ch.ma Prof.ssa Noemi Baldino

Firma_____ NOEMI BALDINO 25.06.2024 09:52:57 GMT+01:00

Supervisore: Ch.mo Prof. Domenico Gabriele

Firma_____ Domenico Gabriele 25.06.2024 09:56:35 GMT+01:00

Dottoranda: Dott./ssa Ylenia Maria Marchesano

Fima Firma oscurata in base alle linee guida del Garante della privacy

La borsa di dottorato è stata cofinanziata con risorse del Programma Operativo Nazionale Ricerca e Innovazione 2014-202 (CCI 2014IT16M2OP005) Fondo Sociale Europeo, Azione I.1 “Dottorati Innovativi con caratterizzazione Industriale”

Index

Abstract

The environmental benefits of reduced toxic emissions, energy and economic savings, fewer and faster traffic disruptions, and increased safety for pavement operators make cold recycling pavement technologies far more advantageous than conventional reconstruction strategies.

The recycling of asphalt mixes is therefore fundamental to a proper policy of natural resource conservation and "integrated" environmental design.

Ecobases are an excellent cold recycling method because they allow the recycling of existing pavements, i.e. RAP, to be combined with the use of bituminous technology formulations, such as bituminous emulsions. Primarily composed of a bituminous and aqueous phase, these materials are undergoing ongoing research and development to enhance their mechanical performance, aiming to surpass that of traditional hot mix pavements. In addition, several studies, including this PhD thesis, are focused on identifying more environmentally friendly surfactants and achieving a higher pH for emulsion stability by using less acid and making the emulsion more stable, as well as on the identification of fillers capable of replacing those currently used, such as cement, which only provide stiffness, with substances capable of providing load-bearing capacity and flexibility at the same time, to resist the loads that road pavements must withstand today

To this end, interfacial techniques have been demonstrated to be crucial. Interfacial instruments can measure the surfactant power of substances through interfacial tensions and therefore their ability to create emulsions.

The ζ-potential measurements and the observation in cylinders of the emulsions were fundamental for stability monitoring and were consistent with both the interfacial and bulk tests.

Chapter 1

1. Introduction

In the age of digital communication, it is necessary to remember and emphasize how roads are our "physical" means of communication. They allow the passage of vehicles, cars, trucks, motorcycles, and farm machinery; if everyone reflected on this, they would realize that roads allow connection for every sphere that affects our lives, from work to food needs, transportation, efficiency of both the public and the economy and interpersonal relationships.

Thinking about this, it is possible to understand the importance of these infrastructures, not only in their design phase, which is crucial but also in their preservation, which is an important step for the protection of the entire population, as well as raw materials and the environment.

Vehicles on the road today have reached an impressive number of 40.7 million, with an average motorization rate about of 700 cars per 1.000 inhabitants and a traffic density of 85 units per kilometre (the highest in Europe) (Stankevich, 2015).

The not-so-easy problem of traffic management is followed by the problem of how to build road infrastructure and restore it, so one must ask what materials to use and what techniques to adopt. Current environmental protection requirements have increasingly directed the efforts of designers to the construction of works that can coexist in harmony with the surrounding environment. The effort of designers and builders of road infrastructure is strongly oriented toward the identification of appropriate design criteria, construction technologies and related acceptance and production controls that can ensure the mitigation of undesirable and/or harmful phenomena for the environment, but at the same time provide better performance.

Achievement of these goals depends on the appropriate use of both traditional and innovative materials, proper sizing of pavement structures, and properly scheduled maintenance to ensure their preservation. Also considering that the road materials have evolved in recent years to cope with the ever-increasing performance demands; added to this are the demands arising from the new and "integrated design" procedures for road infrastructure. The environmental impact statement (EIS) and the environmental impact assessment (EIA) become design tools not only endowed with their internal consistency but built together with the project, which becomes the primary tool for minimizing impacts. Environmental

protection is no longer just a document to be attached to the project, but becomes an integral part of it, constituting its guiding principle.

In this sense, it is clear that the field of research on this topic includes both asphalt mixes and environmental protection and, most importantly, the interrelationships between them.

It is therefore useful to define the main performance parameters required of asphalt mixes and surface treatments:

- Load capacity;
- Adherence;
- Regularity;
- Drainability;
- Visibility

and those related to the eco-compatibility of the motion and the protection of the environment surrounding

- Noise;
- Vibration;
- Rolling resistance.

The construction, maintenance and upgrading of road infrastructure in general and of asphalt carpets, in particular, involves a high economic outlay and a high demand for valuable raw materials consisting of quarry aggregates.

In the last 50 years, highways have undergone unprecedented development; many of them have been in service for more than two decades and, having reached the end of their useful life, require increasing maintenance efforts to maintain an acceptable level of service. In addition, the average number of vehicles has increased over the years: higher loads and the age of the pavement are all factors that contribute to pavement deterioration.

To address the resulting problems, scientific and technical institutions have developed several new practical techniques and solutions most notably. Cold mix asphalt (CMA) is a low-carbon manufacturing approach to the production of flexible pavement material that has proved to be very promising (Shanbara et al., 2021).

Cold mix asphalt is produced by mixing emulsified bitumen, cutback or foamed bitumen with unheated aggregates.

The reasons supporting cold recycling are many and all equally important from the point of view of environmental protection: reduction in the use of raw materials, and landfill areas, containment of soil and atmospheric pollution due to waste transportation and thus less environmental impact, reduction of energy consumption and emissions drastically reduced by using room-temperature materials to produce and manufacture of CMA (Cardone et al., 2015)

In addition to its environmental benefits, pavement cold recycling technologies provide cheaper, faster, and less traffic disruptions alternative to conventional reconstruction strategies. Moreover, these technologies can lower both paving and service temperatures, reducing toxic emissions and, consequently, safeguarding the environment, and those working in the industry, and bringing economic and environmental advantages.
The recycling of asphalt mixes is therefore of paramount importance for a proper policy of protection of natural resources and "integrated" environmental design. In the two fields of study described, the technical experiences and scientific innovations are numerous, and the correlations between road materials in general and asphalt mixes in particular and the environment are indeed numerous.

This PhD work focused on the study and optimization of one of the more desirable CMAs: cold bitumen emulsion mixture (CBEM). CBEM has a wide range of production temperatures as it usually is manufactured at ambient temperatures under different environmental conditions without heating for both aggregates and bitumen (Shanbara et al., 2021).
Even though CBEM techniques have several advantages when compared to HMA regarding ecological, production and economic objectives, it is not without fault (Dulaimi, Al Nageim, Ruddock, et al., 2017). These include weak early strength, high void ratios and an increased curing time required to reach full strength. Because of these, various manufacturing and enhanced approaches to the production of these mixtures are currently under development.

2. Bituminous emulsion (BE) and cold bituminous emulsion mixture (CBEM)

Emulsions are dispersed systems consisting of two immiscible liquids. One immiscible liquid is the continuous phase, which contains an internal phase dispersed as small droplets (Querol et al., 2019). Surfactants, which are chemical compounds with surface activity, make such systems possible. When dissolved in the water phase, they reduce the interfacial

tension between immiscible liquids, facilitating the dispersion of one liquid into the other (Yuliestyan et al., 2017).

Specifically speaking, bituminous emulsion consists of the bitumen phase dispersed in a soap solution, stabilized with a surfactant and it represents a way to use bitumen at low temperatures (Querol et al., 2019).

CBEM is the most popular type of CMA mixture. It is used to create a bituminous mixture produced by mixing bitumen emulsion with mineral aggregates (Dulaimi, Al Nageim, Hashim, et al., 2017). The CBEM industry is interested in using either virgin aggregate or RAP (Reclaimed Asphalt Pavement) or both together to gain an optimum gradation.

2.1 Bituminous emulsions composition

In general, bitumen emulsion consists of three main components: bitumen, water and an emulsifying agent. Bitumen is the main component and its amount in the emulsion depends on the emulsion type and its purpose, usually from 50 %w/w-75 %w/w of the emulsion (Hussein et al., 2020). Bitumen grade, or hardness, significantly affects the produced emulsions which are normally manufactured with bitumen in the 40 – 250 penetration grade (Pan et al., 2019).

The second component of bitumen emulsion is water which contains minerals that affect the manufacture of stable bitumen emulsions. Accordingly, water, containing particulate materials, and impure water are not preferred for emulsions as they disrupt the proportion of the emulsion ingredients and can negatively influence behavior or result in untimely breaking (Arafat et al., 2020).

Emulsifiers are surface-active agents, or surfactants, that have a significant impact on the properties of bitumen emulsions. The emulsifiers have a very important role in controlling breaking time due to their ability to keep the bitumen droplets in a stable condition (Thanaya, 2003). Emulsifiers can be cationic or anionic. Fatty acids such as lignins, tall oils and rosins, which are wood-product derivatives, are considered the most anionic emulsifiers. Fatty amines are the most common cationic emulsifiers such as imidazolines, amidoamines and diamines (Thanaya, 2003). Fatty quaternary ammonium salts are another type of emulsifying agent that is utilized to produce cationic emulsions. These types of emulsifiers are adequate and stable cationic emulsifiers as they are water-soluble salts and do not need the addition of acid.

Several factors influence the manufacture, storage and behaviour of bitumen emulsions (Dulaimi, Al Nageim, Ruddock, et al., 2017):

- The base bitumen chemical properties, hardness, quality and particle size in the emulsion;
- Emulsifying agent type, concentration and properties;
- The temperature and pressure used during manufacturing;
- Emulsion particles' ionic charge;
- The order in which ingredients are added;
- Use of additives such as chemical modifiers and polymers.

2.2 Classification of bituminous emulsions

Bituminous emulsions can be classified as anionic, cationic and non-ionic (Arafat et al., 2020). Both anionic and cationic types are the most widely used in the pavement industry and for maintenance. Categorization by type refers to the electrical charges surrounding the bitumen particles. If this electric current is passed through a bitumen emulsion containing negatively charged particles of bitumen, these particles will move to the anode, thus the emulsion is classified as anionic. In contrast, positively charged bitumen particles will migrate to the cathode, the emulsion identified as cationic. Neutral bitumen particles do not move to either pole, the emulsion, in this case, is classified as non-ionic (Thanaya, 2003).

Emulsions are also classified based on the breaking rate, which is the moment when water separates from the bitumen and the setting phenomenon begins. This classification is simplified and standardized by adopting the terms RS (rapid-setting), MS (medium-setting) and SS (slow-setting) (Thanaya, 2003). The RS emulsion has little or no ability to mix with aggregates, the MS emulsion seems to mix with coarse aggregates, while the SS emulsion prefers to mix with coarse and fine aggregates.

In addition to this labelling, bitumen emulsions are identified by using different letters and numbers that indicate their viscosity and the hardness of the base bitumen in accordance with BS EN 13808. The letter “C” at the beginning of the emulsion type indicates that it is cationic. A second letter “B” indicates the binder content. Occasionally, in the case of an added polymer, the third letter included is “P” and also if the emulsion contents flux (more than 2 %w/w), this is the fourth component indicated by the letter “F”. The first number that follows the letter “C” is related to the percentage of binder content in the bitumen emulsion. The other number at the end refers to the breaking rate, ranging between 1 (fastest breaking

rate) to 7 (slowest breaking rate). For instance, C50BPF3 refers to a cationic emulsion with 50 % based bitumen, that contains a polymer and more than 2 % flux, with a class 3 breaking rate (Shanbara et al., 2021). Anionic bitumen emulsions are identified based on the British Standard Institution using three elements (Hussein et al., 2020). The first element refers to the type of emulsion, for example, 'A' for anionic emulsion. The next part represents the stability or breaking value, ranging between 1 to 4, where the higher value refers to a slow breaking rate. The last component of the code indicates the bitumen content in the emulsion. For example, A1-60 is an anionic emulsion with rapid breaking and 60 % emulsion-based bitumen.

2.3 Production of emulsion

There are two different methods of manufacture of bituminous emulsions, the conventional method and the High Internal Phase Ratio (HIPR) method.

Currently, the most widely used system for the manufacture of bitumen emulsions consists of a mechanical colloid mill with a high-speed rotor (about 1000–6000 rotations per minute), which causes a turbulent regime to split the bitumen into very small droplets (*Abbas Al-Hdabi*, 2014). The hot bitumen (at a temperature between 140 and 180 °C) together with the soap phase (at about 40–60 °C) flows through the small opening (<1 mm) in the engine for a very short period. Using this system, emulsions with a residual bitumen concentration between 60 and 70%, an average drop size of 5–50 μm, and wide granulometric distributions are obtained.

The HIPR (High Internal Phase Ratio) method also disperses two immiscible phases. It uses phase inversion that takes into account the physicochemical nature of each component and the proportions of each used during manufacturing. By varying the formulation and the composition of the manufacturing variables, the type of emulsion obtained as well as its properties can be controlled. This method consists of the direct mixing of a very viscous phase, 1–5000 Pa·s at 100 °C, with a second phase, immiscible in the first, and at least one surfactant. A viscoelastic paste is obtained with low shear, in a laminar regime, and in a very short time. This paste can be subsequently diluted to the required dispersed phase concentration. With this system, it is possible to obtain concentrated and highly concentrated emulsions, 70–95 %w/w, stable in storage, with narrow granulometric distribution and small drop size (around 1 μm) (Examiner & Szekely, 2008).

2.4 Emulsion breaking and curing

If the bitumen emulsion is used as a binder to the aggregates in road works, on top of ensuring the emulsion performs optimally, the water should be separated and evaporated from the emulsion. This separation is called "breaking" (Thanaya, 2003). Then the setting occurs, which is the stage in which the bitumen loses the water remaining in it, and tightens more and more around the inert a process that consists of three stages: decantation, flocculation and coagulation of bitumen particles, stages that result in sedimentation, particle rapprochement and fusion of the particles with each other (Querol et al., 2019). When the bitumen disperses the more volatile components it contains, adhesion is complete, and the binder that remains consists only of nonvolatile hydrocarbons.

Depending on the application, bituminous emulsion is formulated to break by one of two breaking mechanisms: chemical and evaporative. The evaporation mechanism is mainly performed for slow-setting emulsion grades, whilst the chemical mechanism is used for breaking medium-setting and rapid-setting grades. The breaking time of rapid-setting emulsions is considerably shorter than the time needed for medium and slow-setting emulsions (Shanbara et al., 2021). The type and concentration of emulsifiers also have an essential role to play in breaking the emulsion. Other factors, explained below, can also control the rate of breaking (*Abbas Al-Hdabi*, 2014).

Curing includes the development of bitumen engineering characteristics. To do this, complete evaporation and absorption of water must be achieved. The particles of bitumen emulsion should join and bond to the intended surface (Serfass et al., 2004). Petroleum solvents can be used in some bitumen emulsions to help in the mixing and coating process, however, the time taken to cure will be influenced by the quantity and type of the solvents used.

The breaking and curing times of bitumen emulsions are affected by several factors including the temperature of the emulsion and that of the environment, the nature of the aggregates, the size of the dispersed bitumen particles, and the way the work is carried out (Shanbara et al., 2021).

2.5 Performance characteristics of CBEM

Mechanical properties of bituminous pavement including stiffness modulus, permanent deformation and fatigue resistance are affected by many factors such as based binder grade

and characteristics, mixture void content, curing time, aggregate characteristics, and additives (Querol et al., 2019).

Despite the significant beneficial environmental and economic impacts of CBEM, in common with other CMA mixtures, it has weaknesses such as insufficient initial stiffness, an extended period of curing and a high level of void ratios, considered substandard to HMA (Shanbara et al., 2021). In contrast to HMA, CBEM requires up to 24 months, in some cases, to attain its eventual strength and related characteristics. As such, cold, humid and rainy weather is considered incompatible with reductions in CBEM curing time. Because of this, CBEM until the last decade has been restricted to reinstatement works, low traffic volume pavements and footways (Thanaya, 2003) (Gómez-Meijide & Pérez, 2014).

Research carried out to examine CBEM's characteristics has identified its main problems and has proposed methods of mitigation. Brown and Needham (Brown & Needham, 2000) noted that adding Ordinary Portland Cement (OPC) to CBEM has positive effects as the mix without OPC, fails at less than 1000 cycles in the unconfined mode of Repeated Load Axial Tests.

Oruc et al. (Oruc et al., 2007) conducted experiments to evaluate the mechanical properties of emulsified asphalt mixtures having 0–6 % Portland cement. Their test results showed significant improvement with high Portland cement addition percentage; moreover, they suggested based on the study test results, that the cement-modified asphalt emulsion mixes might be used as structural pavement layer. Thanaya et al. (Thanaya, 2003) reported the test results of research on cold emulsion mixtures. They showed that the addition of 1–2% rapid-setting cement accelerates the earlier strength as well as improves the mechanical performance of the modified cold mixes.

Other attempts have tried using waste materials and by-products to improve cold mixes, achieving good results on CBEMs. Research works implemented by Thanaya et al. indicated that pulverised fly ash (PFA) can be used as a suitable filler in cold mixes at full curing conditions (Thanaya, 2003). Also, they found that the fully cured stiffness of the cold mix achieved is very comparable to hot mixtures.

Khalid and Eta (Khalid & Eta, 1999) carried out a laboratory investigation to study the impact of polymer-enhanced emulsions on the mechanical properties of emulsified bitumen macadam. They concluded that Styrene-Butadiene-Styrene (SBS) and Ethylene Vinyl

Acetate (EVA) polymers have positive effects on the modification of bitumen emulsion as they enhance stiffness and reduce permanent deformation of CBEMs.

Shanbara et al. (Shanbara et al., 2021) studied the effect of using natural hemp (HEM), jute (JUT), coir (COI) and synthetic glass (GLS) fibers on the rutting performance of CBEM at 60 °C against conventional (CON) CBEM and HMA mixtures. Including these types of fibers as reinforcing materials, has the potential to enhance the overall pavement strength, and to develop cohesion and durability (Ferrotti et al., 2014).

These fibers have a range of desirable properties and are used to reinforce other materials which also require such properties (Fu et al., 2017; Fakhri & Hosseini, 2017). There is a good possibility of developing the bond and tensile strength of hot and cold mixes by using fibers that have better tensile strength, as opposed to bituminous mixes alone (Xue & Qian, 2016). The main objectives of using fibers as reinforcing materials in pavement construction are to develop tensile strength and provide more strain resistance to fatigue cracking and permanent deformation of the resulting mixtures. Draining down of bituminous mixes is prevented by using fibers, rather than polymers, during all pavement construction stages (Park et al., 2015). In addition, fibers improve the viscosity of bituminous mixtures (Fakhri & Hosseini, 2017), resistance to rutting, stiffness modulus, moisture susceptibility and retard reflection cracking for pavements (Moghaddam et al., 2011).

3. Goals of PhD work

CBEM, a promising low-carbon pavement technology with niche applications, needs further development for broader use. Challenges related to its strength also exist, prompting ongoing research to optimize this material. This work aims to optimize this highly promising material. First, we studied an industry-leading CBEM formula to understand its strengths and build upon them. Subsequent optimization targeted three key areas: employing a more environmentally friendly surfactant, minimizing the stabilizing acid content, and substituting cement with a more flexible yet high-performing material. While cement boasts environmental benefits, its curing time and rigidity limit its effectiveness. We opted for citrus fiber, upcycling a food industry byproduct for cold recycling applications. This approach promotes environmental sustainability, offers energy savings, and potentially reduces costs.

Bibliography

Abbas al-hdabi. (2014). *May*.

Arafat, S., Noor, L., Wasiuddin, N. M., & Salomon, D. (2020). Development of a Test Method to Measure RAP Percentage in Asphalt Mixes in the Field Using a Handheld FT-IR Spectrometer. *Journal of Materials in Civil Engineering*, *32*(12), 1–10. https://doi.org/10.1061/(asce)mt.1943-5533.0003442

Brown, S. F., & Needham, D. (2000). Paper offered for the 2000 Annual Meeting of the Association of Asphalt Paving Technologists A Study of Cement Modified Bitumen Emulsion Mixtures Professor S F Brown 1 and Dr D Needham 2. *Association of Asphalt Paving Technologists*, 1–22.

Cardone, F., Grilli, A., Bocci, M., & Graziani, A. (2015). Curing and temperature sensitivity of cement-bitumen treated materials. *International Journal of Pavement Engineering*, *16*(10), 868–880. https://doi.org/10.1080/10298436.2014.966710

Dulaimi, A., Al Nageim, H., Hashim, K., Ruddock, F., & Seton, L. (2017). *Investigation into the stiffness improvement, microstructure and environmental impact of a novel fast-curing cold bituminous emulsion mixture*. *June 2016*. https://doi.org/10.14311/ee.2016.425

Dulaimi, A., Al Nageim, H., Ruddock, F., & Seton, L. (2017). High performance cold asphalt concrete mixture for binder course using alkali-activated binary blended cementitious filler. *Construction and Building Materials*, *141*, 160–170. https://doi.org/10.1016/j.conbuildmat.2017.02.155

Examiner, P., & Szekely, P. (2008). *(12) United States Patent*. *2*(12).

Fakhri, M., & Hosseini, S. A. (2017). Laboratory evaluation of rutting and moisture damage resistance of glass fiber modified warm mix asphalt incorporating high RAP proportion. *Construction and Building Materials*, *134*, 626–640. https://doi.org/10.1016/j.conbuildmat.2016.12.168

Ferrotti, G., Pasquini, E., & Canestrari, F. (2014). Experimental characterization of high-performance fiber-reinforced cold mix asphalt mixtures. *Construction and Building Materials*, *57*, 117–125. https://doi.org/10.1016/j.conbuildmat.2014.01.089

Fu, Z., Shen, W., Huang, Y., Hang, G., & Li, X. (2017). Laboratory evaluation of pavement performance using modified asphalt mixture with a new composite reinforcing material. *International Journal of Pavement Research and Technology*, *10*(6), 507–516. https://doi.org/10.1016/j.ijprt.2017.04.001

Gómez-Meijide, B., & Pérez, I. (2014). A proposed methodology for the global study of the mechanical properties of cold asphalt mixtures. *Materials and Design*, *57*, 520–527. https://doi.org/10.1016/j.matdes.2013.12.079

Hussein, Z. H., Yaacob, H., Idham, M. K., Hassan, N. A., Choy, L. J., & Jaya, R. P. (2020). Restoration of Aged Bitumen Properties Using Maltenes. *IOP Conference Series: Materials Science and Engineering*, *713*(1). https://doi.org/10.1088/1757-899X/713/1/012014

Khalid, H. A., & Eta, K. E. (1999). Permanent deformation characteristics of bituminous emulsion macadams. *Proceedings of the Institution of Civil Engineers: Transport*, *135*(2), 103–111. https://doi.org/10.1680/itran.1999.31376

Moghaddam, T. B., Karim, M. R., & Abdelaziz, M. (2011). A review on fatigue and rutting performance of asphalt mixes. *Scientific Research and Essays*, *6*(4), 670–682.

Oruc, S., Celik, F., & Akpinar, M. V. (2007). Effect of cement on emulsified asphalt mixtures. *Journal of Materials Engineering and Performance*, *16*(5), 578–583. https://doi.org/10.1007/s11665-007-9095-2

Pan, C., Liang, D., Mo, L., Riara, M., & Lin, J. (2019). Influence of different modifiers on bonding strength and rheological performance of bitumen emulsion. *Materials*, *12*(15). https://doi.org/10.3390/ma12152414

Park, P., El-Tawil, S., Park, S. Y., & Naaman, A. E. (2015). Cracking resistance of fiber reinforced asphalt concrete at -20 °c. *Construction and Building Materials*, *81*, 47–57. https://doi.org/10.1016/j.conbuildmat.2015.02.005

Querol, N., Barreneche, C., & Cabeza, L. F. (2019). Asphalt emulsion formulation: State of the art of formulation, properties and results of HIPR emulsions. *Construction and Building Materials*, *212*, 19–26. https://doi.org/10.1016/j.conbuildmat.2019.03.301

Serfass, J. P., Poirier, J. E., Henrat, J. P., & Carbonneau, X. (2004). Influence of curing on cold mix mechanical performance. *Materials and Structures/Materiaux et Constructions*, *37*(269), 365–368. https://doi.org/10.1617/14130

Shanbara, H. K., Dulaimi, A., Al-Mansoori, T., Al-Busaltan, S., Herez, M., Sadique, M., & Abdel-Wahed, T. (2021). The future of eco-friendly cold mix asphalt. *Renewable and Sustainable Energy Reviews*, *149*. https://doi.org/10.1016/j.rser.2021.111318

Stankevich, A. (2015). *Master ' s Thesis platforms Master ' s Thesis*. *3189214*, 1–77.

Thanaya, I. N. A. (2003). *IMPROVING THE PERFORMANCE EMULSION OF COLD BITUMINOUS (CBEMs) INCORPORATING WASTE The University of Leeds School of Civil Engineering*. *July*.

Xue, Y., & Qian, Z. (2016). Development and performance evaluation of epoxy asphalt concrete modified with mineral fiber. *Construction and Building Materials*, *102*, 378–383. https://doi.org/10.1016/j.conbuildmat.2015.10.157

Yuliestyan, A., García-Morales, M., Moreno, E., Carrera, V., & Partal, P. (2017). Assessment of modified lignin cationic emulsifier for bitumen emulsions used in road paving. *Materials and Design*, *131*(February), 242–251. https://doi.org/10.1016/j.matdes.2017.06.024

Chapter 2

1. Introduction

In the last decades, researchers have improved both pavement construction procedures and material selection intending to obtain perpetual pavements. They have analysed different failure mechanisms and their causes and investigated the mix procedures of materials chosen, along with their quantities. These last play a crucial role in how asphalt pavements respond to the ever-increasing demands of traffic. As a result, different types of pavement failure arise from the interaction of material selection and the stresses inflicted by heavier traffic loads. When pavement condition deteriorates to an unacceptable level, applying reasonable rehabilitation methods becomes necessary to restore its performance. Cold recycling stands out as one such method and a popular choice for its numerous benefits. In addition to its environmental benefits, pavement recycling technologies offer a cheaper, faster, and less disruptive alternative to conventional reconstruction strategies (Alkins et al., 2008). These technologies can further benefit the environment and workers by lowering both paving and service temperatures, thereby reducing toxic emissions. Overall, cold recycling offers a compelling combination of economic and environmental advantages.

Cold bitumen emulsion mixture is one of the most famous and extensively used techniques because of its low environmental impact (Al-Hdabi & Al Nageim, 2017). It is a dispersion of bitumen in a water solution with an anionic or cationic emulsifying agent. An emulsifier is a surface-active agent with hydrophilic and lipophilic groups in the molecule and it can reduce the interfacial tension between the phases to form a stable asphalt emulsion (Querol et al., 2017) In relation to the type of emulsifier used, the emulsion will also be named anionic or cationic. Cationic emulsions are the most commonly used and this is due to the ability of the emulsifier to adhere to electronegative siliceous solid aggregates, the most common mineral used (Yuliestyan et al., 2017).

The amount of bitumen in the emulsion depends on the emulsion type and its purpose, usually from 57% w/w to 63% w/w and then the purpose of the correct addition of the emulsifier is important because promotes the dispersion of the two phases, preventing the agglomeration of particles, charging them electrically and promoting emulsion stability by the repulsive effect induced by surface charges.

These mixes, however, have shown inferior characteristics such as weak earlier-life mechanical properties and high porosity compared with hot mix asphalt (Al Nageim et al., 2012). In the light of above, research is aimed at improving the mechanical performance of these mixtures, in terms of stiffness modulus, permanent deformation and fatigue resistance. All these requirements are affected by many factors such as base binder grade and characteristics, mixture void content, curing time, aggregate characteristics, and additives (Al-Hdabi & Al Nageim, 2017).

Attempts to improve the mechanical properties of cold mixes have been investigated. With the addition of 1%w/w Portland cement compared with untreated mixes (Wang & Sha, 2010). Oruc et al. (2007) conducted experiments to evaluate the mechanical properties of emulsified asphalt mixtures having 0 – 6% Portland cement (Oruc et al., 2007).
Other attempts tried the use of waste and by-product materials to improve cold mixes such as steel slag, PFA (a fluoropolymer with properties similar to polytetrafluoroethylene), crushed glass and used cylinder oil (Pouliot et al., 2003). Theoretically, four main benefits can be achieved when utilizing the by-product materials on CBEMs (Cold Bituminous Emulsion Mixtures): absorption of the trapped water via the hydration process, improvement in mixture mechanical properties, cost-effectiveness and the ecological benefit factor.

Depending on the applications for which they are intended, bituminous emulsions differ in breaking rate: fast, medium and slow breaking emulsions. In particular, fast-breaking emulsions are used for tack coats (Albayati et al., n.d.).

In order to understand the breaking of bitumen emulsions, it is necessary to define precisely what is meant by “breaking”. When the water and binder particles are separated and the particles are merged again, producing a bituminous film, the emulsion is broken and it is largely used for surface treatment, such as slurry surfacing, reinstatement work on low trafficked, walkways, tack coating and cold recycling (Raposeiras, 2013).

The breaking process of the bitumen emulsion is initiated when put into contact with aggregates when processing road surfacing: it is due to interactions with them and water loss (evaporation and gravity flow). Some mechanisms supposed to play a role in the breaking process, like emulsifier adsorption at minerals surface, rise in pH or ionic species release have been studied (Boucard et al., 2015).

In light of the above, the challenge of emulsion is generally manipulated by selecting the appropriate components, surfactant, bitumen, aqueous phase, mechanical variables of mixing and their quantities. The optimized emulsion should provide a formulation with stability and breaking time suitable for its use, and able to ensure adequate coating of the aggregate (Al-mohammedawi & Mollenhauer, 2022).
For this reason, it is essential to identify the right surfactant, studying its emulsifying capacity by studying its interfacial properties.

Three emulsifiers were studied in this paper, two of which are industrial (Cetyltrimethylammonium Chloride and Redicote E11), and one is a potential, more eco-sensitive substitute (Guar-Gam Esaflor®). The first, used by the Valli-Zabban company, Cetyltrimethylammonium Chloride (CTAC, Cationic surfactant, C19H42ClN), is a cationic emulsifier, and it has excellent stability and biodegradability. It has good compatibility with cationic, nonionic, and zwitterionic surfactants and it is widely used in asphalt emulsification and water-proof coating emulsification (Wu et al., 2022).
Polyamines REDICOTE E11, a valid industrial competitor, is a liquid emulsifier for bitumen road cationic emulsions with a slow decay rate, and its recommended concentration in the water phase is 0.6 – 1.5%w/w (Solodkyy et al., 2012). Finally, Guar-Gam Esaflor®, a natural polysaccharide commonly used as a thickening and gelling agent (Thombare et al., 2016), functionalised was used. This last emulsifier could become an interesting alternative to traditional emulsifiers. Specifically speaking, Guar-Gam Esaflor® is a range of guar gum ethers, consisting of cationic and non-ionic hydroxy alkylated products**.**

After having identified the best steps to obtain an emulsion closer to an industrial emulsion, this work aimed to study the interfacial behaviour of surfactants at the interface with bitumen, to replace or optimise the surfactant, first by studying another industrial competitor, then by looking for a more environmentally friendly solution. Kinetic analysis of interfacial mechanism was investigated. Furthermore, the emulsion was prepared and studied in terms of viscosity and stability.

2. Materials and Methods

2.1 Materials

An industrial emulsion (EI), kindly provided by Valli Zabban S.r.l., was used as a reference in this study. REDICOTE E11, provided by Nouryon (Sweden), Guar-Gam Esaflor

(Marchemical Lab. S.r.l (Italy)) and Cetyltrimethylammonium Chloride (CTAC, M.W. = 320 g/mol) were used as emulsifiers to realise laboratory emulsions.

Deltafluid (Marchemical Lab. S.r.l (Italy) was used as the bitumen solvent and Milli-Q distilled water (Millipore Corp.) for interfacial characterization, while a virgin bitumen with penetration grade 50/70 was kindly supplied by Valli Zabban S.r.l (Italy) and used for all the emulsions and investigations. Distillate water was used to prepare emulsions and chloridric acid (37%w/w) (Titolchimica, Italy).

2.2 Sample preparation for interfacial analysis

Deltafluid was used as a solvent for the bitumen dilution to perform the interfacial analysis because of the high viscosity of the bitumen at 25°C. Different solvent/bitumen ratios were investigated to choose the optimum ratio (70, 60, 55, 50, 45, 40, 30 and 20% w/w deltafluid/bitumen). The diluted bitumens at different ratios were studied by both interfacial characterization and bulk analysis. Blend samples are identified by the first letter of solvent (deltafluid) and bitumen, followed by a number representing the weight percentage of solvent in the solution (e.g., the 70% w/w of the blend is identified as 70%_D/B). The ratio 50/50 w/w was chosen as the optimum for the interfacial characterization of the surfactant solutions.

The solutions obtained by adding the emulsifier to Milli – Q ultrapure water are identified as soap solution (SS). All the SSs were prepared by dissolving under stirring the correct amount of surfactants in Milli-Q ultrapure water (Millipore, USA). The solutions were stirred for twenty minutes by a magnetic stirrer (AREX Heating Magnetic Stirrer, Velp Scientifica, Italy) at 50°C. Finally, the pH was adjusted by adding the correct amount of chloridric acid to reach the different pH levels: 2.5, 4.5 and 6.8.

All the SSs, obtained with surfactants and at different pH, were analyzed in the range between 2.5% to 10^{-4} % w/w, to obtain the adsorption isotherms at the diluted bitumen/water interface.

Samples analyzed were reported in Table 1.

ID	Solvent	Surfactant type	pH
SS_C_pH2.5	Milli – Q ultrapure water	CTAC	2.5
SS_C_pH4.5	Milli – Q ultrapure water	CTAC	4.5
SS_C_pH6.8	Milli – Q ultrapure water	CTAC	6.8
SS_G_pH2.5	Milli – Q ultrapure water	GUAR	2.5
SS_G_pH4.5	Milli – Q ultrapure water	GUAR	4.5
SS_G_pH6.8	Milli – Q ultrapure water	GUAR	6.8
SS_R_pH2.5	Milli – Q ultrapure water	REDICOTE E11	2.5
SS_R_pH4.5	Milli – Q ultrapure water	REDICOTE E11	4.5
SS_R_pH6.8	Milli – Q ultrapure water	REDICOTE E11	6.8
SS_CG_pH2.5	Milli – Q ultrapure water	CTAC-GUAR	2.5

Tab.1: Sample ID of the studied SS.

It is important to emphasize that in SS_CG_pH2.5 guar replaces 10% of the total surfactant, which is the maximum usable percentage in terms of solubility and viscosity, chosen following various tests. Thus, in the case of 1.2% w/w of SS_CG, i.e., there is 1.1% w/w of CTAC and 0.1% w/w of Guar-gum esaflor®.

2.3 Emulsion preparation

Bituminous emulsion was prepared by homogenization of two phases:

- soap solution (aqueous phase),
- bitumen phase.

The soap solution (SS) was prepared as described in Section 2.2. The base bitumen was heated in a laboratory oven (BINDER, Germany) at 130°C for 1 h.

The two phases were then mixed by emulsification with an Ultraturrax T50 (IKA-WERKE, Germany) equipped with a G45F tool, at 7600 rpm for four minutes. The final temperature of the emulsion was 90°C.

Emulsions analyzed were reported in Table 2.

ID	**Surfactant type**	**Guar** **% (w/w)**	**CTAC** **% (w/w)**	**Redicote E11** **% (w/w)**
ECG_0.1-1.1_pH2.5	CTAC-GUAR	0.1	1.1	0
ECG_0.1-1.1_pH4.5	CTAC-GUAR	0.1	1.1	0
ECG_0.1-1.1_pH6.8	CTAC-GUAR	0.1	1.1	0
ER_1.2_pH2.5	REDICOTE E11	0	0	1.2
ER_1.2_pH4.5	REDICOTE E11	0	0	1.2
ER_1.2_pH6.8	REDICOTE E11	0	0	1.2
EI_1.2_pH2.5	CTAC	0	1.2	0
EIL_1.2_pH2.5	CTAC	0	1.2	0
EIL_1.2_pH4.5	CTAC	0	1.2	0
EIL_1.2_pH6.8	CTAC	0	1.2	0

Tab.2: ID emulsions analyzed.

Surfactant content in emulsions is measured by weight and is calculated with respect to the total weight of the samples.

2.4 Sample preparation for ζ-potential

Samples for ζ-potential analysis were prepared by dissolving 1 ml of emulsion in 250 ml of distilled water acidified with chloridric acid at pH of the emulsion under test and dispersed with the help of a magnetic stirrer (AREX Heating Magnetic Stirrer, Velp Scientifica, Italy) for ten minutes according to the methodology proposed in the literature (Pinto & Buss, 2020).

2.5 Methods

2.5.1 Interfacial analysis

Dynamic interfacial tensions have been measured with a pendant drop tensiometer (FTA200, First Ten Angstroms, USA). In this technique, a drop is formed at the end of a syringe tip in a glass cell filled with the second phase, the drop is imaged with a video camera and analyzed with a computer program that solves the Laplace equation describing mechanical equilibrium under capillary and gravity forces and allows monitoring of the interfacial tension variation with time (Arashiro & Demarquette, 1999).

For the measurements, the diluted bitumen was pumped in a syringe (100 µl glass Hamilton, 1710TLL) equipped with a j-needle and the drop was formed in the surfactant solution put in a couvette. After drop formation at the water interface, its profile was monitored during the time at constant volume. The drop profile was monitored and the equilibrium surface tension, γ_{eq}, was determined for all the tested samples at all the different concentrations, assuming that the equilibrium is reached when the tension did not change by more than 0.5 mN/m during 30 min (Seta et al., 2012).

Three replicates for each sample were prepared independently and tested. All samples were characterized within 24 h and the results are shown as average value and standard deviation. All experiments were performed at room temperature (25 °C) and atmospheric pressure. Data fitting was carried out by using Origin 2019b (OriginLab Corporation, USA).

The main consideration when discussing IFT data is the application of an appropriate isotherm. The goal of the adsorption isotherm is to relate the bulk concentration and the composition at the interface. According to Pradilla and Eastoe, the Gibbs equation provides a model based on thermodynamics (Eastoe & Dalton, 2000; Pradilla, 2016). Assuming that activities may be given by concentrations (dilute solutions), the surface excess may be obtained from Eq.1:

$$\Gamma = -\frac{1}{\mathrm{n}RT} \cdot \frac{d\gamma}{dln(c)} \qquad \text{Eq.1}$$

Here Γ is the equilibrium surface excess, n is a constant, in particular, n= 1 for non-ionic surfactants, neutral molecules or ionic surfactants in the presence of excess electrolyte, and n=2 for 1:1 ionic surfactants, assuming electrical neutrality of the interface (Navarro, 1998). R is the gas constant, T is the Kelvin temperature, γ the surface/interfacial tension and c is the bulk surfactant concentration. The Γ *vs.* c curve can be obtained by fitting an adequate set of data adsorption.

The most commonly and widely used non-linear adsorption isotherm is that of Langmuir. It is a two-parameter equation and it is based on the assumption that:

- every adsorption site is equivalent;
- there are no interactions between the adsorbed species;
- the molecules are adsorbed as a monolayer (Pradilla, 2016)

A simple approach for describing adsorption is described next. The rate of change of surface coverage due to adsorption is proportional to both the concentration of surfactant in solution, and the number of vacant sites available. The maximum number of sites available is Γ_∞

$$\frac{d\Gamma}{dt} = k_c \cdot c \cdot \Gamma_\infty \cdot \left(1 - \frac{\Gamma}{\Gamma_\infty}\right) \qquad \text{Eq.3}$$

The rate of Γ change , due to desorption is proportional to the number of adsorbed species:

$$\frac{d\Gamma}{dt} = k_d \cdot \Gamma \qquad \text{Eq.4}$$

At equilibrium, these two rates are equal, and introducing the Langmuir equilibrium adsorption constant K_L=k_{ads}/k_{des}, results in the Langmuir isotherm,

$$\Gamma = \Gamma_\infty \cdot \left(\frac{k_L C}{1+k_L C}\right) \qquad \text{Eq.5}$$

where Γ_∞ is the surface excess at saturation and k_L is known as the adsorption constant. It is a two-parameter equation.

The analogous equation of state is known as the Szyszkowski equation, reported in Eq.6:

$$\pi = nRT\Gamma_\infty ln(1 + k_L C) \qquad \text{Eq.6}$$

In which π is the surface pressure or the difference in IFT between a clean interface, for instance, that of a pure solvent and the value when the surface-active agents have been adsorbed.

Deviations from the Langmuir isotherm may be attributed to the failure of the assumption of equivalent and independent sites (Eastoe & Dalton, 2000).

2.5.3. Adsorption kinetics

The well-known Ward-Tordai equation is widely used to model adsorption kinetics limited only by diffusion of surfactants towards an interface. It allows the calculation of diffusion coefficients based on the interfacial tension data. As the IFT decays, this model accounts for how the molecules are being diffused and subsequently adsorbed onto the interface. There are two main mechanisms included in this model. First, at short times and with a fresh interface the monomers will adsorb directly, thus it is assumed that every molecule arrives at an empty site. Second, with the molecules present at the oil-water interface, back diffusion takes place, this means that the molecules that arrive at an already occupied site will return to the bulk (Eastoe & Dalton, 2000). The equation in its usual form cannot be solved, therefore asymptotic solutions have been proposed. When the short-time approximation is used, the measured interfacial tension will be close to that of the pure solvent; hence it can be assumed that the solution is dilute. When this happens, the Henry isotherm can be applied, and the diffusion coefficient can be obtained from the following equation (Pradilla, 2016):

$$\gamma_{t\to 0} = \gamma_0 - 2nRTC_0\sqrt{\frac{Dt}{\pi}} \qquad \text{Eq.7}$$

In this equation, D is the diffusion coefficient of the adsorbing molecule, γ_0 is the interfacial tension of pure solvent and C_0 is the concentration in the bulk.

According to Eq.7, for a diffusion-controlled process, γ_t should vary linearly with $t^{0.5}$. Therefore, to better analyze the adsorption kinetics IFT vs. $t^{0.5}$ may be plotted and the slope as the linear correlation between γ_t and $t^{0.5}$ in Eq. (7) is defined as k (Zhang et al., 2018)

$$k = 2RT\sqrt{\frac{D}{\pi}}C_0 \qquad \text{Eq.8}$$

Finally, the coefficient D can be derived. The interfacial diffusion coefficient D is related to k by Eq.9 (Zhang et al., 2018)

$$D = \pi \left(\frac{k}{2RTC_0}\right)^2 \quad \text{Eq.9}$$

2.5.2 Rheological analysis

Dynamic Shear Rheological (DSR) measurements on bitumen/solvent blends were carried out using a controlled shear stress rheometer (Haake Mars III, Thermo Fisher Scientific, Germany), equipped with a titanium parallel plate (P5, Φ = 50mm, polished, gap=1 ± 0.1 mm) and with a Peltier system for temperature control. Flow curves, in the range between 0.1 to 500 s^{-1}, were performed for all the analyzed samples.

2.5.3 ζ-potential and stability analysis of emulsion samples

A ζ - potential analyzer (Zetasizer Nano ZSP, Malvern Panalytical Ltd, UK) was used to achieve the charge analysis of the emulsions. Couvette DTS1070 was used for all tests. The measurements require an equilibrium time of 120 seconds. Measurements were performed in triplicate.

Stability was also monitored and analyzed through:

- Optical observation in the graduated cylinder during the time (0 - 2h);
- Centrifugation (sedimentation emulation)

For effective optical observation, the percentage of foam in the cylinders is read and the percentage of the latter to the total is derived using Eq.7 defined as the ratio between the height of the foam at t=0 (Hfoam) and the total height of the emulsion (Htot) (Lajnaf et al., 2022):

$$\%H_{foam} = \frac{H_{foam}}{H_{tot}} \cdot 100 \quad \text{Eq.10}$$

For the sedimentation test, instead, according to Latreille and Paquin (LATREILLE & PAQUIN, 1990), the emulsion was centrifugated for 1, 3 and 5 min at 1600 rpm, by centrifuge (5810, Eppendorf, Germany) and the volume of surfactant was measured.

3. Results

3.1 Interfacial analysis

The adsorption isotherms of CTAC at the DB/SS interface are reported in Fig.1 and it is possible to observe a typical sigmoidal trend at all the pH levels.

As already mentioned, the dilution was necessary to perform the interfacial analysis because of the high viscosity of the bitumen at 25°C, but it is important to emphasize that the results obtained can be attributed to those of a pure bitumen with all the endogenous surfactant species, i.e. asphaltenes and resins, and all other species, even if diluted then with a lower concentration.

As reported in the model systems in the literature (Zhang et al., 2018), dilution can affect the equilibrium value of the tension and the adsorption kinetics in terms of value, but not in terms of behaviour. In the system under study, however, dilution acts on the entire bitumen system, without modifying the composition and relationships between the naturally present species.

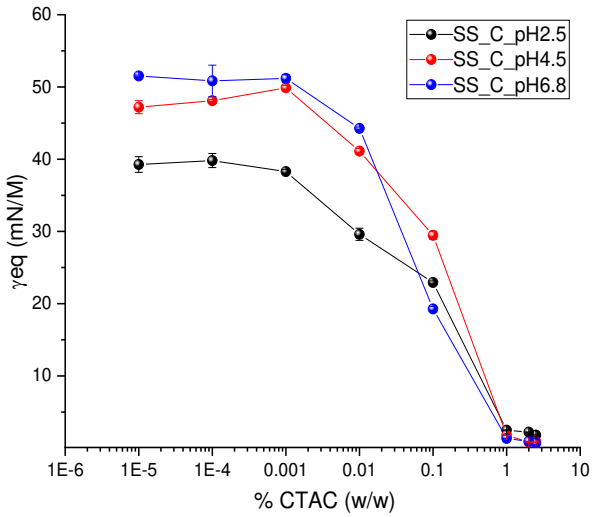

Fig.1: Adsorption isotherms of CTAC at SS/DB interface at pH=2.5, 4.5 and 6.8.

The adsorption isotherms, in Fig.1, indicate that IFT decreases with increasing surfactant concentration for all three pH investigated. SS_C_pH2.5 sample shows the lowest IFT on average, but after the concentration of 1% w/w the values are higher than the other two samples. Literature suggests that the increase in acidity, and thus freer H^+ ions, polarizes

more of the endogenous surfactants in bitumen, i.e. asphaltenes and resins (Benderrag et al., 2016), and the effect is an IFT decrease with pH decrease (Fig.1).

As surfactant concentration increases, it is evident (Fig.1) that IFT of SS_C decreases at all pH levels; moreover, it is found a cross of hydrophilicity around 0.03% CTAC w/w (and the tension increases as the pH decreases, as shown in the detail of Fig. 2). This is generally attributed to a co-adsorption and therefore to a competitive effect at the interface of the native surface-active components present in the bitumen and the added cationic surfactant ionized at low pH (Poteau et al., 2005).

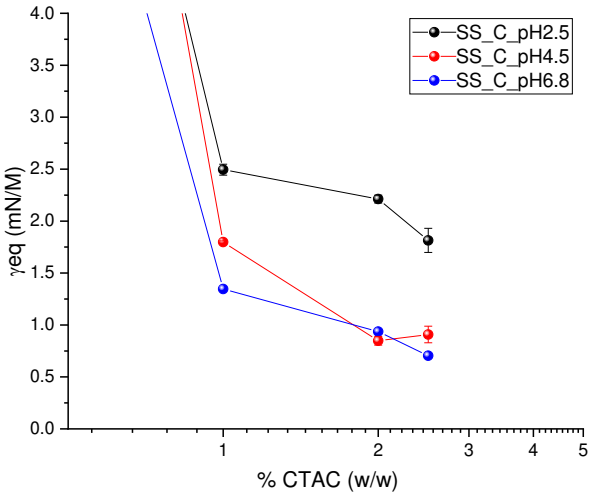

Fig.2: Detail at high concentrations of surfactant of adsorption isotherms of CTAC at SS/DB interface at pH=2.5, 4.5 and 6.8.

Moreover, the literature suggests that ideal emulsifying agents are amphoteric materials, so the charge acquired at low pH (cationic) and high pH (anionic) increases their hydrophilic behaviour and makes them more surface-active (Dickinson, 2003). Consequently, in the case of CTAC, cationic surfactant, the interfacial film formed should act as a more efficient barrier to prevent the water droplet coalescence at pH=2.5 than at pH=6.8.

It is also important to underline that for use in slow-breaking emulsions it is preferable to work at CMC, which is obvious when the drops are completely solvated.

The obtained results are consistent with the stability as also predicted by the cylinder stability test and z-potential shown later.

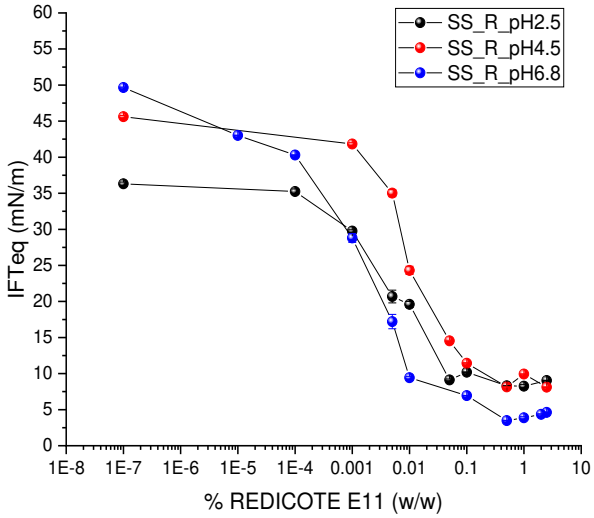

Fig.3: Adsorption isotherms of REDICOTE E11 at SS/DB interface at pH=2.5, 4.5 and 6.8.

REDICOTE E11, as shown in Fig.2, exhibits the same tension trend of CTAC as a function of concentration, but has a lower ability to reduce IFT compared to it, because it is a fatty amine and therefore has a lower surfactant capacity than a powerful emulsifier such as CTAC, which is a quaternary ammonium salt. The difference between the various surfactants depends on different types of hydrophilic groups (Logaraj et al., 2000).

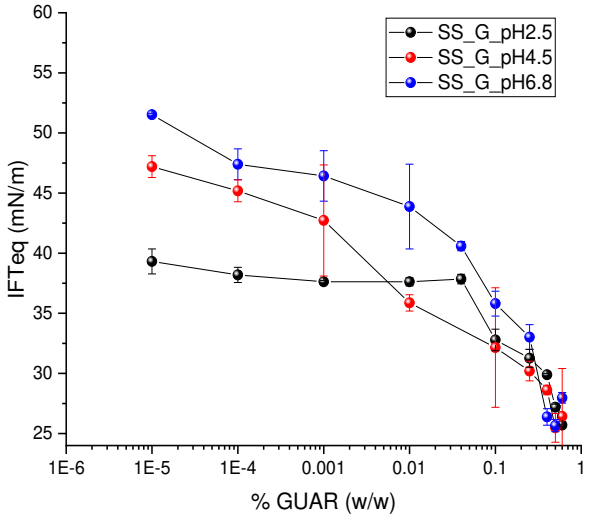

Fig.4: Adsorption isotherms of GUAR-GAM ESAFLOR at SS/DB interface at pH=2.5, 4.5 and 6.8.

Finally, guar reaches equilibrium levels, but as a polysaccharide, and therefore a biopolymer, reaches modest levels compared to a cationic surfactant.

For a biopolymer to be surface-active, it clearly must have amphiphilic character. So, if it is a hydrocolloid, it must contain hydrophobic groups that are numerous enough and sufficiently accessible on a short timescale to enable the adsorbing molecules to adhere to and spread out at the interface, thereby protecting the newly formed droplets. Hence, an ideal emulsifying agent, capable of making small droplets, is typically composed of species of relatively low molecular mass with good solubility in the aqueous continuous (Dickinson, 1994).

The limited emulsifying capacity of some biopolymers can be attributed to poor solubility and/or insufficient amphiphilic character to produce a rapid and substantial lowering of the interfacial tension during droplet breakup. Irrespective of the degree of amphiphilic character, though, the large molecular mass of a typical hydrocolloid makes it an unlikely candidate for an ingredient of the very highest emulsifying ability (Dickinson, 2003).

The interfacial analysis of the individual isotherms shows that the best-performing surfactants are CTAC and REDICOTE E11. Even if GUAR does not have a high surfactant power, it was used as a co-emulsifier, replacing CTAC even at low percentages, which ensures solubility. Three different levels of SS_CG_pH2.5 were studied and the IFT values are shown in Tab.3

SS_CG_pH2.5	
%CTAC-GUAR	**IFT [mN/m]**
2.5	1.54 ± 0.13
1.1	2.71 ± 0.16
1	2.76 ± 0.03
BIANCO	39.31 ± 1.04

Tab.3: IFT of equilibrium of SS_CG_pH2.5.

As shown in Tab.3, concentrations from CMC upward were analyzed, because the prevailing character and thus behaviour is given by CTAC, so it was useless to analyze again a wide range of concentrations.

It is important to report and analyze, at this time, the Szyszkowski isotherm parameters for each surfactant, as well as its diffusion parameters, to understand which surfactant is faster, i.e., capable of lowering IFT in a shorter time, and more efficient.

pH=2.5	**γ_∞ [N/m]**	**Γ_∞ [mol/m^2]**	**k_L [m^3/mol]**
SS-C	0.039±0.001	1.21E-6±1.01E-7	8908 ± 100
SS-G	0.038±0.001	1.66E-6±4.79E-7	141.23 ± 27
SS-R	0.033±0.001	5.18E-07±3.22E-09	360000 ± 73000

Tab.4: Langmuir parameters for SS_C, SS_G and SS_R at pH=2.5.

pH=4.5	**γ_∞ [N/m]**	**Γ_∞ [mol/m^2]**	**k_L [m^3/mol]**
SS-C	0.050 ± 0.002	1.80E-6 ± 1.64E-7	4206 ± 200
SS-G	0.047 ± 0.002	5.21E-7 ± 4.70E-8	118000 ± 1300
SS-R	0.044 ± 0.001	8.18E-7 ± 2.44E-7	316000 ± 360

Tab.5: Szyszkowski parameters for SS_C, SS_G and SS_R at pH=4.5.

pH=6.8	**γ_∞ [N/m]**	**Γ_∞ [mol/m^2]**	**k_L [m^3/mol]**
SS-C	0.051 ± 0.002	1.63E-6 ± 1.50E-7	10499.87±7101.37
SS-G	0.048 ± 0.001	1.28E-6 ±1.54E-7	1470.08±716.40
SS-R	0.044 ± 0.002	8.18E-7 ± 7.52E-8	330000 ± 850

Tab.6: Szyszkowski parameters for SS_C, SS_G and SS_R at pH=6.8.

Tab. 4, 5 and 6 summarize the equilibrium parameters using the Szyszkowski Isotherm.

The values γ_∞ for SS-C, SS-G and SS-R are consistent, at all three pHs, with the results of the adsorption isotherms in Figs.1 and 3. In fact, this value should represent the value at very low surfactant concentrations, close to the reference blank for each pH, and as visible in Tabs.4, 5 and 6 is exactly what is obtained from Szyszkowski Isotherm fitting.

Γ_∞, is the surface excess at saturation, therefore, the amount of surfactant adsorbed at equilibrium (Pradilla, 2016). The rate of change of surface coverage due to adsorption is proportional to both the concentration of surfactant in solution, and the number of vacant sites available. The maximum number of sites available is Γ_∞ (Eastoe & Dalton, 2000). shown in Tabs. 4,5 and 6, values of Γ_∞ are greater for CTAC and guar because, having a lower molecular weight than redicote, it follows that the molecules adsorbed, and in particular the surface excess at saturation, at the same area, is greater.

K_L is known as the adsorption constant and is related to the molecular weight of the surfactant, so the larger it is the greater K_L will be. This is consistent with results reported in Tabs. 4, 5 and 6; in fact, the highest K_L is that of Redicote, followed by guar up to CTAC, almost for all pHs. This is therefore inversely proportional to the surface excess at saturation, based on what was just mentioned above.

As mentioned earlier, to better analyze the adsorption kinetics IFT vs. $t^{0.5}$ may be plotted and the slope as shown in Fig. 4.

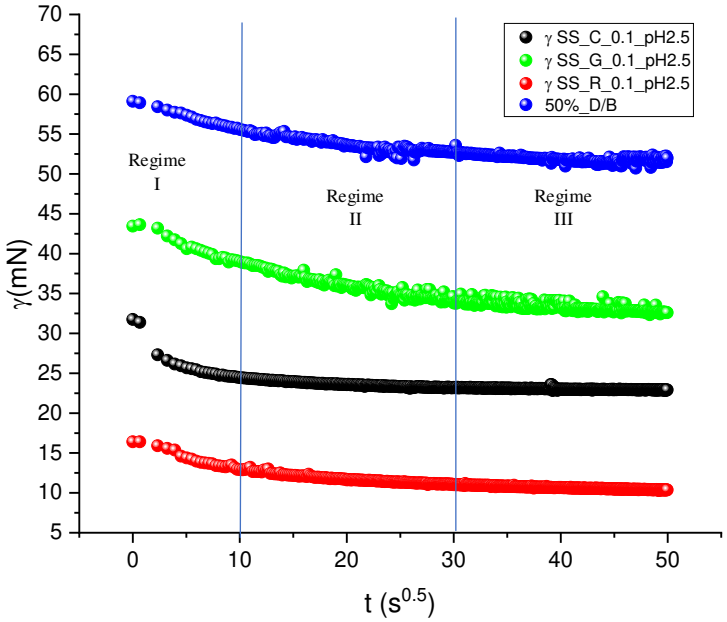

Fig.5: IFT vs $t^{0.5}$ of SS with various surfactants at 0.1% and 50%_DB

Fig. 4, according to Shuo Zhang et al. 2018 clearly shows that the adsorption process of surfactants to the oil/water interface can be divided into three stages separated by the dash lines, denoted as Regime I, Regime II and Regime III, respectively from left to right. Regime I is the initial stage which shows the sharpest reduction of IFT with time (Zhang et al., 2018). Regime III is the stage at a relatively long time that gradually approaches adsorption equilibrium. Regime II is the transition stage between Regimes I and III, where the curve slope falls between that of Regimes I and III

Based on Fig. 4, the slopes of the linear fitting of the IFT data in Regime I can be directly obtained. Consequently, D can be calculated as suggested by Eq.9.

SS-C	**pH=2.5**	**pH=4.5**	**pH=6.8**
% ($w_{surf}/w_{solution}$)	**D [m^2/s]**	**D [m^2/s]**	**D [m^2/s]**
0.1	1.50E-09 ± 6.9E-10	7.75E-09 ± 1.28E-09	4.62E-09 ± 2.35E-09
0.01	3.10E-08 ± 5.5E-09	1.18E-07 ±6.27E-08	4.89E-07 ± 4.61E-08
0.001	1.50E-05 ± 2.5E-06	1.58E-05 ± 2.98E-06	1.75E-05 ± 4.61E-06

Tab.7: Diffusion coefficient, D, for SS_C at varying concentrations and pH.

SS_G	**pH=2.5**	**pH=4.5**	**pH=6.8**
% ($w_{surf}/w_{solution}$)	**D [m^2/s]**	**D [m^2/s]**	**D [m^2/s]**
0.1	9.29E-10 ± 1.64E-10	5.16E-09 ± 1.10E-09	2.42E-09 ± 3.92E-10
0.04	1.09E-09 ± 4.97E-10	1.67E-08 ± 8.21E-13	3.98E-09 ± 8.43E-10
0.01	6.35E-08 ± 2.77E-10	2.96E-07 ± 1.68E-07	8.57E-08 ± 3.24E-10
0.001	3.03E-06 ± 2.84E-06	4.19E-05 ± 4.30E-05	4.40E-06 ± 6.63E-07

Tab.8: Diffusion coefficient, D, for SS_G at varying concentrations and pH.

SS-R	pH=2.5	pH=4.5	pH=6.8
% ($w_{surf}/w_{solution}$)	D [m^2/s]	D [m^2/s]	D [m^2/s]
0.01	1.51E-07 ± 1.90E-09	1.94E-07 ± 1.17E-07	2.53E-07 ± 1.11E-07
0.005	7.67E-07 ± 4.05E-08	2.02E-06 ± 3.38E-08	9.43E-07 ± 2.73E-07
0.001	1.13E-06 ± 2.70E-07	1.20E-05 ± 2.01E-08	3.97E-05 ± 2.07E-05

Tab.9: Diffusion coefficient, D, for SS_R at varying concentrations and pH.

Tabs. 7, 8 and 9 summarize the values of the diffusion coefficients calculated using equation 9.

The diffusion coefficient calculated for the three SS at different surfactant concentrations and pH, using Equation 9, is reported only for the concentrations shown in Tabs 7, 8 and 9. because at higher concentrations the values were too small, and as suggested by Pradilla values too low denote that the adsorption is not diffusion-controlled (Pradilla, 2016). However, a reference of molecules with similar molecular weight reports values for the diffusion coefficient of $D \sim 10^{-10}$ m^2/s (Eastoe & Dalton, 2000).

Values of D shown in Tabs. 7, 8 and 9 are consistent for all surfactants at varying pH in that it increases as concentration decreases, and this is due to the concentration gradient between the bulk and the interface: when the interface is still empty the surfactant tends to move rapidly toward it, decreasing when it is reaching saturation. As reported by Shuo Zhang, while under a fixed temperature, increasing surfactant concentration leads to a lower interfacial diffusion coefficient because the sites at the interface are occupied more quickly as the bulk concentration increases (Zhang et al., 2018).

3.2 Rheological analysis

Flow curves were run on various the mix of deltafluid/bitumen (D/B) at different w/w to ensure the correct viscosity for the interfacial tests.

Naturally, the system of interest is bitumen/SS, but the very high viscosity of bitumen makes it impossible to place bitumen in the syringe at room temperature for interfacial analysis.

To facilitate bitumen injection, a hydrocarbon diluent, Deltafluid (D), was identified. This diluent reduces bitumen viscosity to a suitable level for syringe application. Different mixtures with different percentages of diluted bitumen were therefore prepared to determine the minimal dilution required to carry out the test.

Figure 4 shows the only blends from the lowest possible reduction to the desired viscosity.

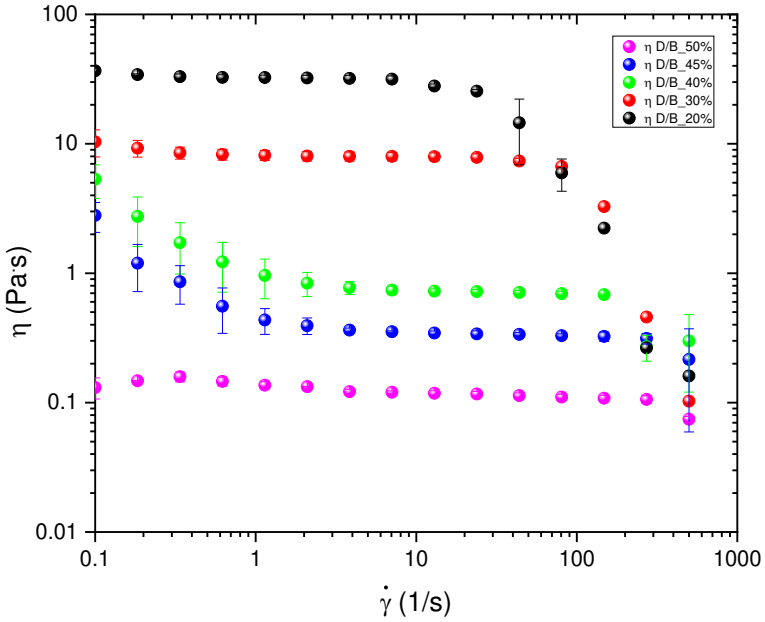

Fig.6: Flow-curve of the ratio 20, 30, 40, 45 and 50%_D/B ($\dot{\gamma}$= 0.1-500 s^{-1});

As seen in Fig.5, the shear thinning behavior of η as a function of shear rate decreases with increasing dilution, and reaches a Newtonian behavior for the D/B50% mixture and a value of 0.1 Pa·s, justifying its use in the syringe. According to laboratory experience with interfacial systems of this type. the maximum achievable viscosity pumped into the syringe to perform the interfacial analysis is 0.1 Pa.s

3.3 Cylinder stability, forced destabilization and ζ-potential

The emulsion stability by cylinder observation and zeta potential measurements are important tests able to identify the best surfactant, as well as monitor the effect of pH to best formulate the desired emulsion.

Cylinder stability was important for the correct laboratory reproduction of EI, so the monitoring obviously concerned EI_1.2, EIL_1.2 and ECG_0.1-1.1 at the three pH analyzed,

while there was no interest in seeing what happened to another industrial emulsifier such as REDICOTE.

Fig.7 and 8 show, respectively, the cylinder stability and forced destabilization of the industrial emulsions EI_1.2_pH2.5. The monitoring process lasted two hours and the creaming value was evaluated every fifteen minutes, but for better understanding only the images at the start and end times are shown.

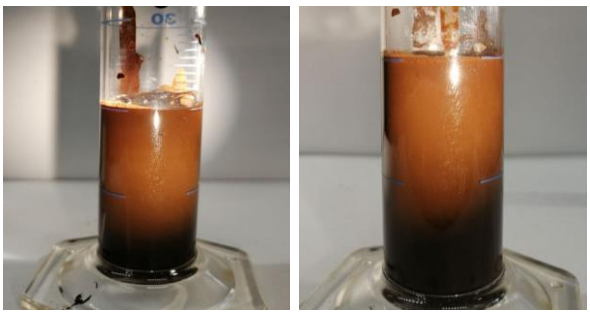

Fig.7: Cylinder stability of EI_1.2_pH2.5, at t_0 and t_f

As clearly visible from Fig.7, the industrial emulsion maintains excellent stability during the monitored time, with no separation and with a distinct light brown color, indicating excellent emulsification. The bitumen has completely emulsified with the soap solution.

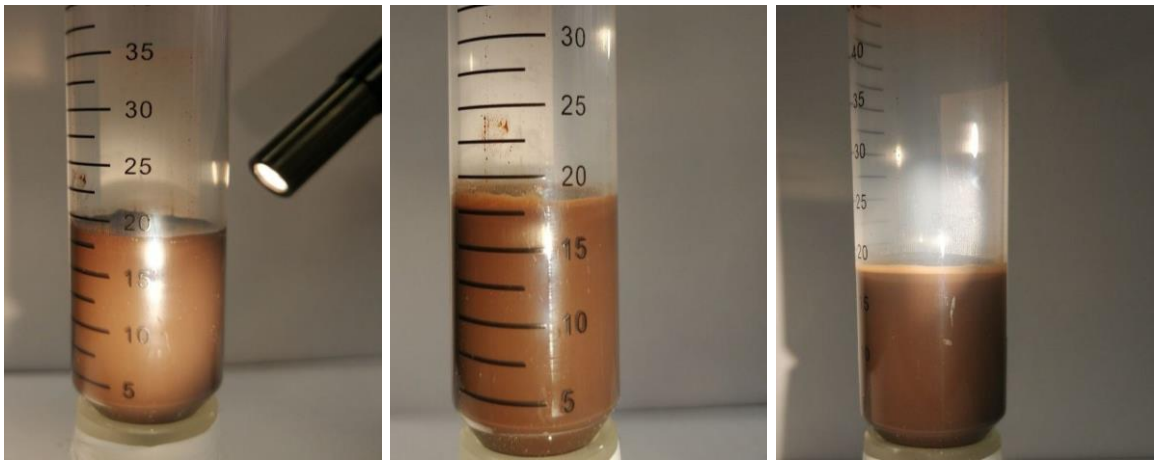

Fig.8: Forced destabilization of V at pH= 2.5 at 1, 3 and 5 minutes.

It is also clear from the forced destabilization, Fig.8, that only after the maximum time among those chosen, i.e. 5 minutes, is there a very low percentage of creaming. It is important to emphasize, however, that this is not an instability, but only a temporary separation (typical of the thermodynamic instability that characterizes emulsions), which immediately reverts to emulsion when the system is stirred.

Then, all the emulsions reported in section 2.2 have been reproduced. Since the emulsification process is different, they are obviously characterized by foam, which is evaluated by Equation 7.

Fig.9 shows EIL_1.2_pH2.5 at t_0 and t_f, just so that the similarity to industrial is visually recognized. The color is light brown, a symptom of an excellent emulsification process because it means, precisely, that all the bitumen has gone into an emulsion with water and there are no black parts

Fig.9: Cylinder stability of EIL_1.2_pH2.5, at t_0 and t_f

Monitoring was performed for the three pH levels and since the foam height does not vary with pH it was not reported.

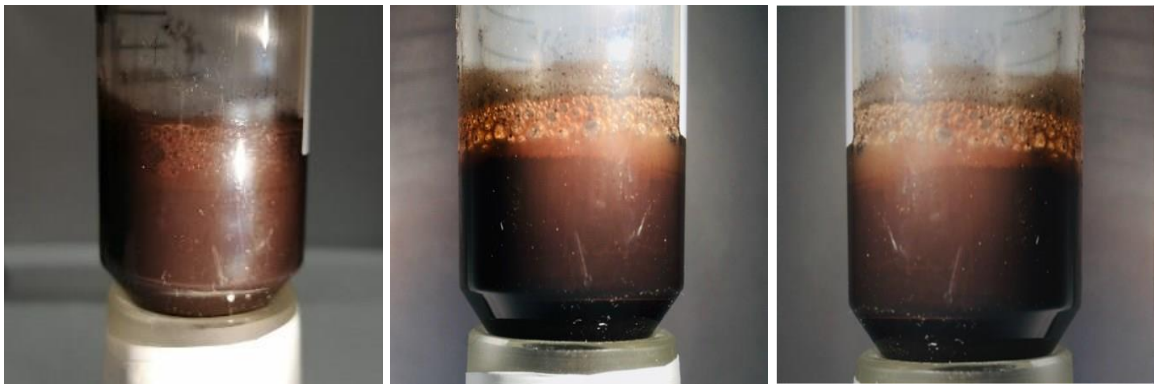

Fig.10: Forced destabilization of EIL_1.2 at pH= 2.5

The destabilization shown in Fig.10, also shows very good breaking strength, although a sharper separation is achieved at t_f than EI_1.2_pH2.5.

The three pH levels were also analyzed for this technique, and it was found that evolution over time does not vary with the pH level.

Therefore, ζ-potential analysis was performed on EI_1.2_pH2.5 and EIL_1.2 at the three pH considered.

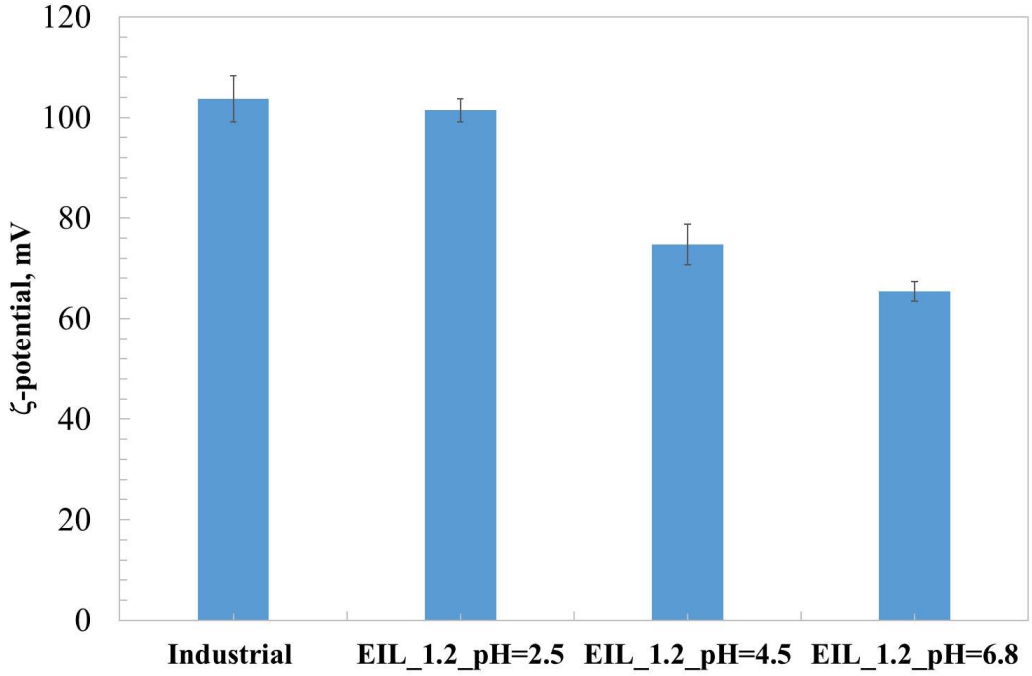

Fig.11: ζ-potential evaluation of industrial emulsion and EIL_1.2 at varying pH.

According to the literature, the ζ-potential values reported in Fig. 11 suggest excellent of all the emulsions obtained because of the value between 60 and 100 mV (Pinto & Buss, 2020). It can also be observed that the ζ-potential value decreases increasing the pH and that in terms of stability, the sample obtained in the laboratory is the same as the industrial one. Moreover, the trend suggests that it is possible to modulate the stability, and therefore the breakage, of this type of emulsion by varying the pH.

Because of the previous results, the stability analysis of the emulsion obtained with Guar was performed only at pH = 2.5, as the industrial emulsion. Subsequently, the cylinder stability, the forced destabilization and the ζ-potential of CG were analyzed at pH=2.5.

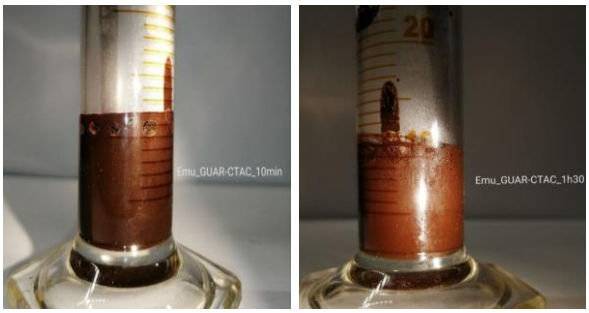

Fig.12: Cylinder stability of ECG_0.1-1.1_pH=2.5 at t_0 and t_f.

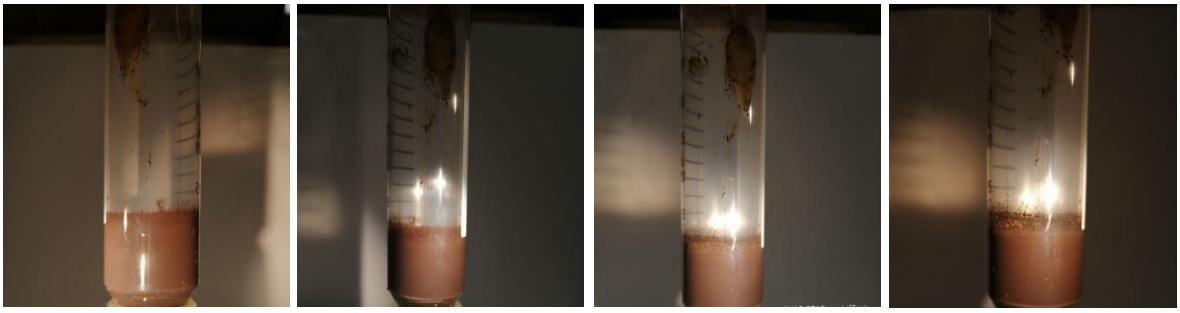

Fig.13: Forced destabilization of CG at pH= 2.5 at 1, 3, 5 and 7 minutes.

As can be seen in Fig.13, forced destabilization also had to be carried out at 7 minutes because at 5 minutes there was still no clear break-up as was the case with VL.

At 7 minutes it can be clearly seen that the water in the emulsion has separated to form a clear, albeit cloudy, level. The need for further forced destabilization is related to the capacity of the GUAR, typically used as a gelling and thickening agent Thombare et al., 2016).

It was mentioned previously that the evaluation of foam height was done by Equation 10. To better understand the values obtained for emulsions monitored, these have been reported in Fig.14.

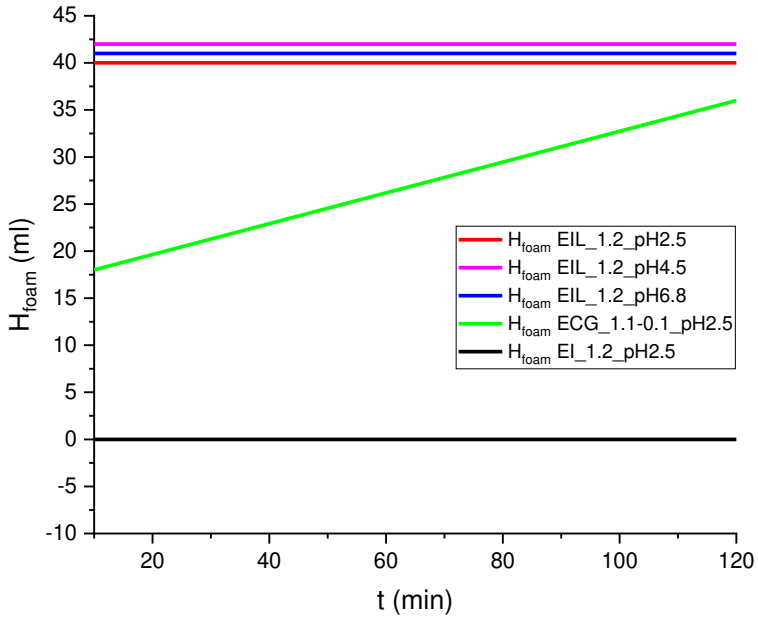

Fig.14: Evaluation of H_{foam} over time of EIL_1.2 at varying pH, ECG_1.1-0.1_pH2.5 and EI_1.2_pH2.5

In Fig.14, EI_1.2_pH2.5 represents the benchmark, and as clearly visible it is set at zero because being industrial and not obtained in the laboratory, it has no foam.
EIL_1.2 and ECG_1.2 reproduced in the laboratory have foam due to the emulsification process as mentioned above.
However, it is interesting to observe that for EIL_1.2 there is no change in foam height over time and, most importantly, there is almost complete similarity among the three pH values analyzed, so that one can speak of invariance compared to pH for stability in cylinders.
ECG_1.2_pH2.5, prepared at this pH for the reasons explained above, shows a time dependence of the foam height. It is most likely that the addition of guar created more foam in the system and the emulsion tends to settle over time.

A more detailed analysis of measuring the ζ potential can help to define a trend regarding the stability of the emulsions analyzed.

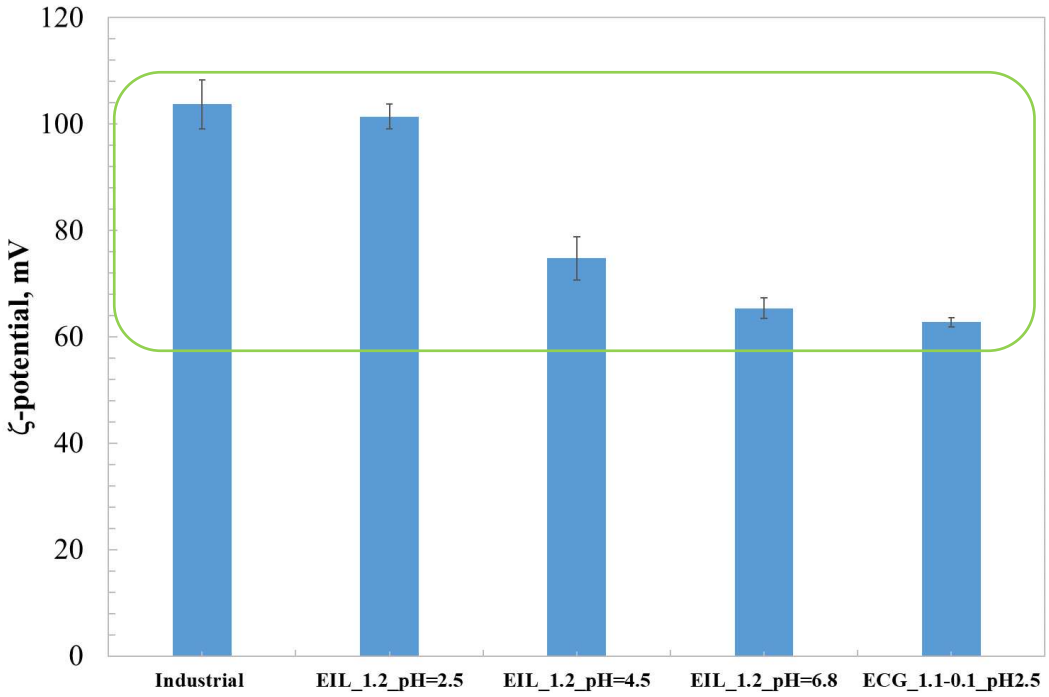

Fig.15: ζ-potential evaluation industrial emulsion, EIL_1.2 at varying pH and ECG_1.1-0.1_pH2.5.

ζ potential (Fig.15) shows that CG is still within the range of excellent stability, so, in addition to making an environmental contribution, it can maintain excellent system stability, providing a valid alternative to industrial emulsion in a more sustainable way.

In conclusion, it can be said that the values of IFT, Γ and ζ potential are important parameters because they predict the rheological behavior of emulsions.

The interfacial tension, IFT, between two species must be low to promote emulsification, a characteristic of surfactant species (Dickinson, 2003), as seen for the surfactants analyzed in Figs. 1,3 and 4. Low IFT confers good bulk properties.

Γ, related to Γ_∞, and so to the amount of surfactant adsorbed at equilibrium (Pradilla, 2016) is another indication of stability, which affects the bulk properties.

The ζ potential, finally, is a potential generated by an electrical double layer responsible for the stability of colloidal systems. As seen in the literature for cationic surfactants, and in particular for bituminous emulsions, it must be above a certain value (Pinto & Buss, 2020) that is reached by all the emulsions analyzed.

For the emulsions analyzed, as can be seen from the results in this chapter, these parameters are consistent and converge in the same direction for all the emulsifiers analyzed.

Bibliography

Al Nageim, H., Al-Busaltan, S. F., Atherton, W., & Sharples, G. (2012). A comparative study for improving the mechanical properties of cold bituminous emulsion mixtures with cement and waste materials. Construction and Building Materials, 36, 743–748. https://doi.org/10.1016/j.conbuildmat.2012.06.032

Albayati, A., Wang, Y., Wang, Y., & Haynes, J. (n.d.). A Sustainable Pavement Concrete using Warm Mix Asphalt and Hydrated Lime Treated Recycled Concrete Aggregates.

Al-Hdabi, A., & Al Nageim, H. (2017). Improving Asphalt Emulsion Mixtures Properties Containing Cementitious Filler by Adding GGBS. Journal of Materials in Civil Engineering, 29(5), 1–7. https://doi.org/10.1061/(asce)mt.1943-5533.0001859

Alkins, A. E., Lane, B., & Kazmierowski, T. (2008). Sustainable pavements environmental, economic, and social benefits of in situ pavement recycling. Transportation Research Record, 2012(2084), 100–103. https://doi.org/10.3141/2084-11

Al-mohammedawi, A., & Mollenhauer, K. (2022). Current Research and Challenges in Bitumen Emulsion Manufacturing and Its Properties. Materials, 15(6). https://doi.org/10.3390/ma15062026

Arashiro, E. Y., & Demarquette, N. R. (1999). Use of the pendant drop method to measure interfacial tension between molten polymers. Materials Research, 2(1), 23–32. https://doi.org/10.1590/s1516-14391999000100005

Benderrag, A., Daaou, M., Bounaceur, B., & Haddou, B. (2016). Influence of pH and cationic surfactant on stability and interfacial properties of algerian bitumen emulsion. Chemical Papers, 70(9), 1196–1203. https://doi.org/10.1515/chempap-2016-0061

Boucard, L., Schmitt, V., Farcas, F., & Gaudefroy, V. (2015). Bitumen emulsions formulation and destabilisation process relationship: influence of salts addition. Road Materials and Pavement Design, 16(May), 330–348. https://doi.org/10.1080/14680629.2015.1030910

Dickinson, E. (1994). Emulsions and droplet size control. In Controlled Particle, Droplet and Bubble Formation. Butterworth-Heinemann Ltd. https://doi.org/10.1016/b978-0-7506-1494-8.50012-2

Dickinson, E. (2003). Hydrocolloids at interfaces and the influence on the properties of dispersed systems. Food Hydrocolloids, 17(1), 25–39. https://doi.org/https://doi.org/10.1016/S0268-005X(01)00120-5

Eastoe, J., & Dalton, J. S. (2000). Dynamic surface tension and adsorption mechanisms of surfactants at the air-water interface. Advances in Colloid and Interface Science, 85(2), 103–144. https://doi.org/10.1016/S0001-8686(99)00017-2

Jiang, H., Zhang, J., Sun, C., Liu, S., Liang, M., & Yao, Z. (2018). Experimental assessment on engineering properties of aged bitumen incorporating a developed rejuvenator. Construction and Building Materials, 179, 1–10. https://doi.org/10.1016/j.conbuildmat.2018.05.211

Lajnaf, R., Picart-Palmade, L., Attia, H., Marchesseau, S., & Ayadi, M. A. (2022). Foaming and air-water interfacial properties of camel milk proteins compared to bovine milk proteins. Food Hydrocolloids, 126(May 2021), 107470. https://doi.org/10.1016/j.foodhyd.2021.107470

LATREILLE, B., & PAQUIN, P. (1990). Evaluation of Emulsion Stability by Centrifugation with Conductivity Measurements. Journal of Food Science, 55(6), 1666–1668. https://doi.org/10.1111/j.1365-2621.1990.tb03595.x

Logaraj, S., Ernzen, T., Lin, M., Hays, T., & Stegemoeller, C. (2000). Emulsification A solution to Asphaltene Handling Problems. ISSA/AEMA 2nd Joint Conference, 12.

Navarro, L. (1998). Gibbs, Einstein and the foundations of statistical mechanics. Archive for History of Exact Sciences, 53(2), 147–180. https://doi.org/10.1007/s004070050025

Oruc, S., Celik, F., & Akpinar, M. V. (2007). Effect of cement on emulsified asphalt mixtures. Journal of Materials Engineering and Performance, 16(5), 578–583. https://doi.org/10.1007/s11665-007-9095-2

Pinto, I., & Buss, A. (2020). ζ Potential as a Measure of Asphalt Emulsion Stability. Energy and Fuels, 34(2), 2143–2151. https://doi.org/10.1021/acs.energyfuels.9b03565

Poteau, S., Argillier, J. F., Langevin, D., Pincet, F., & Perez, E. (2005). Influence of pH on stability and dynamic properties of asphaltenes and other amphiphilic molecules at the oil-water interface. Energy and Fuels, 19(4), 1337–1341. https://doi.org/10.1021/ef0497560

Pouliot, N., Marchand, J., & Pigeon, M. (2003). Hydration Mechanisms, Microstructure, and Mechanical Properties of Mortars Prepared with Mixed Binder Cement Slurry-Asphalt Emulsion. Journal of Materials in Civil Engineering, 15(1), 54–59. https://doi.org/10.1061/(asce)0899-1561(2003)15:1(54)

Pradilla, D. (2016). Asphaltenes and Asphaltene model compounds: Adsorption, Desorption and Interfacial Rheology. https://brage.bibsys.no/xmlui/handle/11250/2383810

Querol, N., Barreneche, C., & Cabeza, L. F. (2017). Method for controlling mean droplet size in the manufacture of phase inversion bituminous emulsions. Colloids and Surfaces A: Physicochemical and Engineering Aspects, 527(May), 49–54. https://doi.org/10.1016/j.colsurfa.2017.05.018

Raposeiras, A. C. (2013). Construc tion and Buildi ng Materia ls Test methods and influential factors for analysis of bonding between bituminous pavement layers. Construction and Building Materials, 43, 372–381. https://doi.org/10.1016/j.conbuildmat.2013.02.011

Sergiy SOLODKYY 1 Iurii SIDUN 2 Oleksiy VOLLIS 3 ACIDS IN BITUMEN EMULSIONS. (n.d.). https://doi.org/10.7862/rb.2018.45

Seta, L., Baldino, N., Gabriele, D., Lupi, F. R., & De Cindio, B. (2012). The effect of surfactant type on the rheology of ovalbumin layers at the air/water and oil/water interfaces. Food Hydrocolloids, 29(2), 247–257. https://doi.org/10.1016/j.foodhyd.2012.03.012

Thombare, N., Jha, U., Mishra, S., & Siddiqui, M. Z. (2016). Guar gum as a promising starting material for diverse applications: A review. International Journal of Biological Macromolecules, 88, 361–372. https://doi.org/10.1016/j.ijbiomac.2016.04.001

Wang, Z., & Sha, A. (2010). Micro hardness of interface between cement asphalt emulsion mastics and aggregates. Materials and Structures/Materiaux et Constructions, 43(4), 453–461. https://doi.org/10.1617/s11527-009-9502-2

Wu, M., Xu, G., Luan, Y., Zhu, Y., Ma, T., & Zhang, W. (2022). Molecular dynamics simulation on cohesion and adhesion properties of the emulsified cold recycled mixtures. Construction and Building Materials, 333(July 2021), 127403. https://doi.org/10.1016/j.conbuildmat.2022.127403

Yuliestyan, A., García-Morales, M., Moreno, E., Carrera, V., & Partal, P. (2017). Assessment of modified lignin cationic emulsifier for bitumen emulsions used in road paving. Materials and Design, 131(February), 242–251. https://doi.org/10.1016/j.matdes.2017.06.024

Zhang, S., Zhang, L., Lu, X., Shi, C., Tang, T., Wang, X., Huang, Q., & Zeng, H. (2018). Adsorption kinetics of asphaltenes at oil/water interface: Effects of concentration and temperature. Fuel, 212(September 2017), 387–394. https://doi.org/10.1016/j.fuel.2017.10.051

Chapter 3

1. Introduction

The most important factors related to bituminous emulsion manufacture are discussed in this chapter.

Emulsions are dispersed systems consisting of two immiscible liquids, one of which is the continuous phase, which contains an internal phase, dispersed as small droplets (Querol et al., 2017). Surfactants, which are chemical compounds with surface activity, make such systems possible. When dissolved in the water phase, they reduce the interfacial tension between immiscible liquids, facilitating the dispersion of one liquid into the other (Yuliestyan et al., 2017)

For the preparation of bituminous emulsions, bitumen in water, there are different methods and procedures. In particular, however, the one that uses colloidal mills is widely used as an industrial process. The mill operates at high temperatures and pressures, 140 - 170 °C and 1 - 3 atm, applying high rotation speeds between 5.000–10.000 rpm, obtaining droplet sizes between 5 and 10 μm can be achieved (Querol et al., 2017).

Another manufacturing system used to disperse two immiscible phases is the HIPR procedure (High Internal Phase Ratio) (James, 2006; Querol et al., 2017), This procedure involves the direct blend of a highly viscous phase, 1–5000 Pa s, with a second phase immiscible on the first one and in the presence of at least one surfactant. It works with low shear, 500–1500 rpm, in laminar flow and very little time, producing a viscoelastic paste which can be subsequently diluted to the required concentration of the dispersed phase. With this system, it is possible to obtain stable storage emulsions with very narrow particle size distribution and small mean droplet size, d (0.5), about 1 μm (James, 2006; Querol et al., 2017).

Particle size and particle size distribution (PSD) are important variables to consider and are controllable with formulation, raw materials, and the equipment used to manufacture the emulsion (James, 2006). The importance of particle size in emulsions has been discussed in many papers (James, 2006). It is a determinant of emulsion stability, coating, break rate, and cure rate.

Methods to improve particle size of emulsions by formulation and adjustment of asphalt chemistry are described in the literature. These methods usually involve improvement of the

dispersing phase, doping of asphalt with surfactants, tailoring asphalt composition and optimization of manufacturing conditions (Querol et al., 2017).

The mean droplet size and the PSD obtained can be controlled by changing the parameters of the formulation such as the volume fraction, concentration and type of surfactant, the temperature of the dispersed phase employed, type of bitumen used, and mechanical variables such as the rotational speed and mixing time used (Querol et al., 2019).

P, which can be single-mode, bi-mode, or multi-mode, is a fundamental element, together with the volume fraction. Monomodal emulsions are characterized by one particle size distribution and therefore more viscous than a multimodal emulsion, with a ϕ_{max}=0.68. Multimodal emulsions, instead, are characterized by having two or more different and controlled droplet sizes and distribution sizes and have a lower viscosity than the monodisperse emulsion, because the ϕ_{max} achievable is 0.8. The optimal formulation contains a first small size of about 1 μm and a second size of about 5 μm with a proportion of 1/2, respectively (James, 2006; Querol et al., 2017).

An interesting parameter of the particle distribution is the Sauter mean $d_{3.2}$ (surface-weighted mean diameter) (Yuliestyan et al., 2016), which is proportional to the surface area dispersed and therefore correlates with viscosity, and the volume-weighted mean diameter, $d_{4.3}$, which is proportional to the largest particles and therefore correlates more with stability (James, 2006).

The type of surfactant used in the manufacture of the emulsion has also a big effect on the speed of the breaking of breaking emulsion.

Emulsified asphalt must revert to a continuous asphalt film to act as a binder in road materials. This involves flocculation and coalescence of the droplets and removal of the water. While evaporation and water absorption can drive setting in very slow-setting emulsions, chemical reactions between the aggregate and the emulsion are the primary mechanism in most cases. The speed of these setting and curing processes depends on the reactivity of the emulsion, the reactivity of the aggregate and environmental factors, such as temperature, humidity, wind speed, and mechanical action. Less viscous asphalts tend to give faster coalescence. It may take a few hours in the case of a chip seal to several weeks in the case of a dense cold mix for the full strength of the road material to be reached (James, 2006).

Stability is essential because it affects the breaking speed and thus determines its application.

During the storage of an emulsion, creaming or sedimentation takes place in the first step. Subsequently, flocculation occurs; it is characterized by the contact between droplets, but they still are partially protected by the film of the emulsifier and, therefore, they maintain their shape. Then coalescence appears in what is already an irreversible process. After the first coalescence, these phenomena are accelerated resulting in the fracture and separation of the phases of the emulsion (Klink et al., 2011). The main factors that influence the storage stability of an emulsion are viscosity and average droplet size (James, 2006).

The viscosity of the emulsion is, therefore, the other very important parameter to consider. In fact, as the viscosity increases, stability also increases, but if the viscosity is too high it will affect the workability. If the viscosity is too high, problems will appear when pumping it from the storage tank to the manufacturing plant, and the wrapping with aggregates will not be correct. The decrease in viscosity that can be observed in bimodal emulsions when compared to equivalent monomodal emulsions can be attributed to the packing of the emulsion droplets (Cardona et al., 2015; James et al., 2017) In bimodal emulsions, the small droplets try to place themselves in the empty voids of the cubic matrix generated by the distribution of the large droplets (Querol et al., 2017) Due to this different packing distribution, the droplet movement should be slower than in monomodal emulsions and, consequently, they have lowered sedimentation rates.

In this work, different emulsifiers were studied at different pH and the preparation process was optimized following the industrial method, not changing the ratio between the two phases and temperatures, while the emulsification parameters, like time and speed, were optimized. The optimization was necessary because of the different emulsification systems, rotor-stator, instead of the colloid mill. Three emulsification speeds were identified from the literature (Querol et al., 2017), 5200, 7600 and 10000 rpm, and optimized by microscopy. The rheological investigation was also performed on the emulsions to understand how the PSD affects the viscosity.

2. Materials and Methods

2.1 Materials

REDICOTE E11, provided by Nouryon (Sweden), Guar-Gam Esaflor (Marchemical Lab. S.r.l (Italy)) and Cetyltrimethylammonium Chloride (CTAC, M.W. = 320 g/mol) were used as emulsifiers to realize laboratory emulsions and compared with an industrial emulsion (EI), kindly provided by Valli Zabban S.r.l. (Italy), was used as a reference in this study. A virgin bitumen with penetration grade 50/70, was kindly supplied by Valli Zabban S.r.l (Italy) and used for all the emulsions and investigations. Distilled water and chloridric acid (37%w/w) (Titolchimica, Italy) were used to prepare emulsions.

2.2 Emulsion preparation

Bituminous emulsion was prepared by homogenization of two phases:

- soap solution (aqueous phase);
- bitumen phase.

The solution obtained by adding the emulsifier to distilled water is identified as soap solution (SS). All the SSs were prepared by dissolving under stirring the correct amount of surfactants in distilled water (Millipore, USA). The solutions were stirred for twenty minutes by a magnetic stirrer (AREX Heating Magnetic Stirrer, Velp Scientifica, Italy) at 50°C. Finally, the pH was adjusted by adding the correct amount of chloridric acid to reach the different pH levels: 2.5, 4.5 and 6.8. The base bitumen was heated in a laboratory oven (BINDER, Germany) at 130°C for 1 h. The two phases were then mixed by emulsification with an Ultraturrax T50 (IKA-WERKE, Germany) equipped with G45F tool at the chosen velocity (5200, 7600 or 10000 rpm) for four minutes. The final temperature of the emulsion was 90°C.

Samples analyzed were reported in Table 1.

ID	Surfactant type	Guar % (w/w)	CTAC % (w/w)	Redicote E11 % (w/w)
ECG_0.1-1.1_pH2.5	CTAC-GUAR	0.1	1.1	0
ECG_0.1-1.1_pH4.5	CTAC-GUAR	0.1	1.1	0
ECG_0.1-1.1_pH6.8	CTAC-GUAR	0.1	1.1	0
ER_1.2_pH2.5	REDICOTE E11	0	0	1.2
ER_1.2_pH4.5	REDICOTE E11	0	0	1.2
ER_1.2_pH6.8	REDICOTE E11	0	0	1.2
EI_1.2_pH2.5	CTAC	0	1.2	0
EIL_1.2_pH2.5	CTAC	0	1.2	0
EIL_1.2_pH4.5	CTAC	0	1.2	0
EIL_1.2_pH6.8	CTAC	0	1.2	0

Tab.1: ID sample analyzed obtained with three different surfactants.

Surfactant content in emulsions is measured by weight and calculated with respect to the total weight of the samples.

2.3 Sample preparation for laser diffraction analysis

To carry out laser diffractometer analysis, the samples were diluted in deionized water in the measuring cell and stirred to avoid interactions between droplets and aggregation phenomena.

2.4 Methods

2.4.1 Rheological analysis

The rheological characterization on bituminous emulsions was carried out using a controlled shear stress rheometer (Haake Mars III, Thermo Fisher Scientific, Germany), equipped with a titanium parallel plate (P50 Ti L, Φ = 50mm, polished, gap=1.0 ± 0.1 mm) and a Peltier

system for temperature control. Specifically, flow curves, in the range between 0.1 to 500 s^{-1} were performed for all the analyzed samples at three temperatures (20°C, 40°C and 60°C) and 2.5, 4.5 and 6.8 of pH.

2.4.2 Laser diffraction analysis

Emulsions were analyzed to determine the droplet size distribution (PSD). Laser diffraction measurements were carried out using a Mastersizer 2000 (Malvern, UK) laser particle size analyzer equipped with a liquid sample dispersion module, Hydro MV (Malvern, UK), which can work between 0.01 to 3500 μm. From the software, the $d_{3.2}$ diameter was obtained only for the emulsions at different rpm while the $d_{4.3}$ was analysed for all the emulsions at different pH and times.

The results shown in this chapter correspond to the average obtained from three measures for each sample. The main droplet size exhibits a deviation between ± 5% and ± 10%.

Measurements were carried out at ambient temperature.

3. Results

3.1 Particle Size Distribution

The first emulsion analysed is the EI_1.2_pH2.5, the industrial emulsion, because used as a reference.

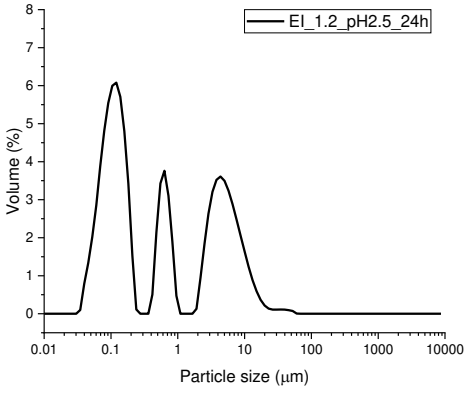

Fig.1: Particle size of industrial emulsion, the EI_1.2_pH2.5, at 24 h.

As shown in Fig.1, the analyzed emulsion is multimodal, with two characteristic picks of bimodal emulsion produced in industrial colloid mills, specifically one starting from 0.3 to 1 µm with a vertex in 0.5 µm, and another from 2 to 10 µm, as reported by (Querol et al., 2017)

A very interesting element in this case, however, is the third peak, with a vertex in 0.1 µm which includes very small particles: this is a demonstration of how, by acting on the parameters mentioned in the introduction, the desired emulsion can be obtained (Querol et al., 2017). The microscopy of sample EI_1.2_pH2.5 shows a higher packing factor, given by particles of different sizes that, going to fit together perfectly, provide very low viscosity and excellent stability (Cardona et al., 2015).

The industrial emulsions, reproduced on a laboratory scale (EIL_1.2_pH2.5) at three emulsification speeds chosen, were analysed over time, specifically at 24 hours, 7 days, 15 days, and 30 days, to determine which of the 3 preparations remained stable over time (Fig. 2).

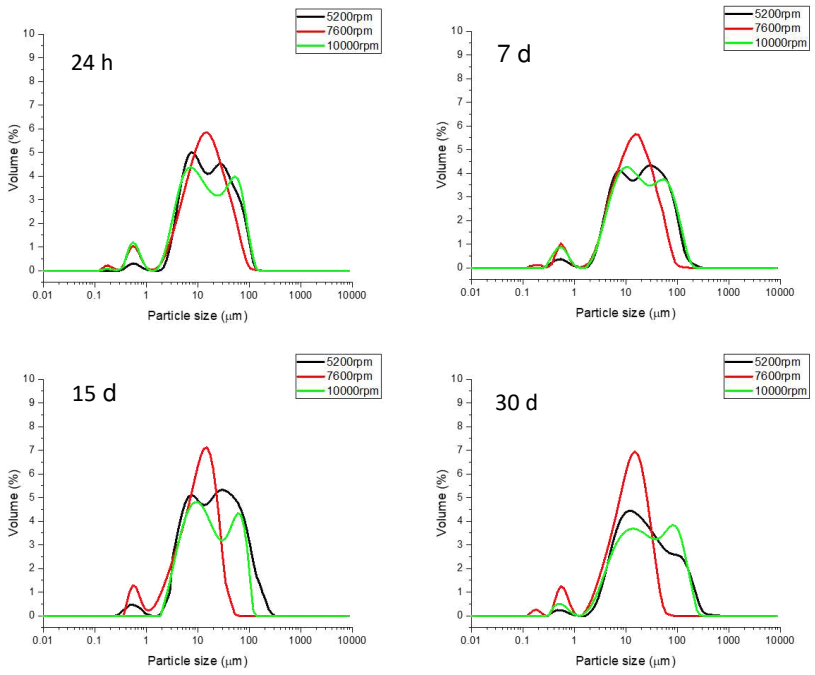

Fig. 2: Evolution of the droplet size distribution over the time of EIL_1.2_pH2.5 at 5200, 7600 and 10000 rpm.

It is clear from Fig. 2 that all emulsification speeds used produce multimodal emulsions, mostly bi-modal, which are therefore characterized mainly by two peaks. Emulsions

obtained at 5200 and 10000 rpm have similar spectrum, characterized by a small peak between 0.3-1 µm but with the main area below the curve from 2 - 200 µm. , which includes many particles of different sizes and changes over time.

In contrast, the sample emulsified at spectrum at 7600 rpm is different, characterized by three peaks, two of which are very small (between 0.1 - 0.3 µm the first two and the predominant between 1-100 µm) and one preponderant. In light of the above, it is evident from Fig. 1 and Fig. 2, that the emulsion prepared at 7600 rpm has a similar behaviour if compared and aldo stability in the medium and long term as also reported in Fig. 3.

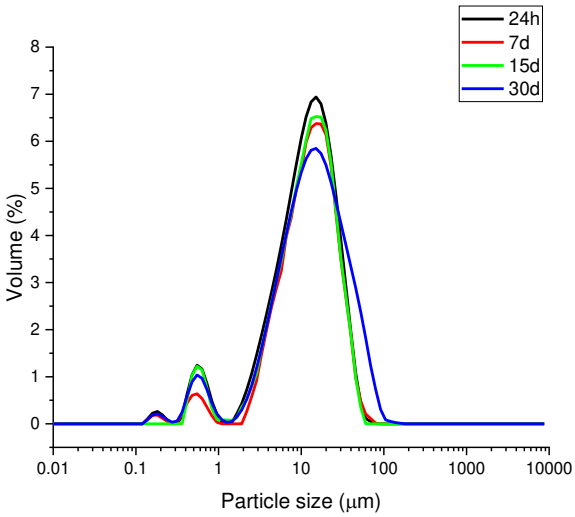

Fig. 3: Evolution of the droplet size distribution over the time of EIL_1.2_pH2.5 at 7600 rpm.

The spectrum reveals a prominent peak with a narrower distribution curve compared to emulsions at 5200 and 10000 rpm. This indicates superior uniformity and stability.

The Sauter diameters, $d_{3.2}$, and $d_{4.3}$, volume-weighted mean diameter, are reported in Table 2 (James, 2006)

RPM	**$d_{3.2}$ [µm]**	**$d_{4.3}$ [µm]**
5200	4.5	27.7
7600	4.3	19.6
1000	5.4	21.2

Tab.2: $d_{3.2}$, and $d_{4.3}$ of EIL_1.2_pH2.5 at 5200, 7600 and 10000 rpm.

As can be seen in Table 2, Sauter diameter $d_{3.2}$ is comparable for all speeds, especially at 5200 rpm and 7600 rpm. Volume-weighted mean diameter $d_{4.3}$, proportional to particle width

and thus stability (James, 2006) instead, at 5200 rpm is very high, a symptom of large particles. It improves markedly at 10000 and 7600 rpm, indicating small particles and therefore better stability.

Therefore, choosing the best emulsification rate based on all the considerations made, the emulsions at pH=2.5 described in section 2.2 were prepared at 7600 rpm, and the effect of time was shown in Fig. 3.

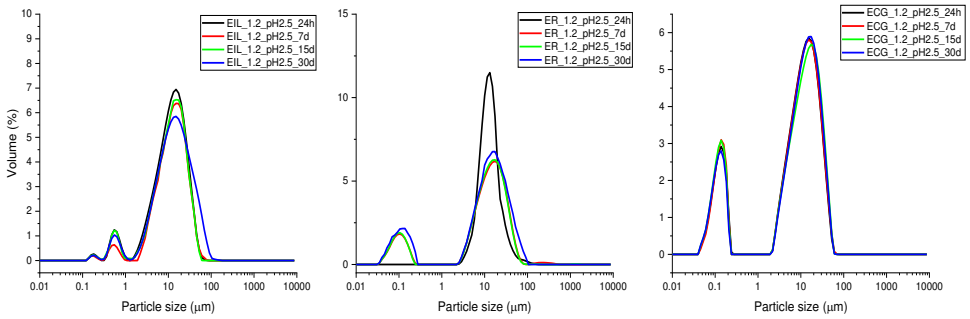

Fig.4: Particle size of EIL_1.2_pH2.5, ER_1.2_pH2.5 and ECG_0.1-1.1_pH2.5 at 1, 7, 15 and 30 days.

The spectra shown in Fig. 4, and especially their evolution over time, confirm that the chosen emulsification method was correct. The emulsions shown in Fig. 4, especially EIL_1.2_pH2.5 and ECG_0.1-1.1_pH2.5, maintain almost the same spectrum from 1 to 30 days.

The emulsion obtained with REDICOTE E11 also shows good stability over time except in the first 24 hours. This initial change can be attributed to lower surfactant power than CTAC. In fact, the interfacial tests carried out in Sec. 3.1 of Chapter 2 shows that REDICOTE E11 has a lower ability to reduce IFT compared CTAC, because it is a fatty amine and therefore has a lower surfactant capacity than a powerful emulsifier such as CTAC, which is a quaternary ammonium salt. The difference between the various surfactants depends on different types of hydrophilic groups (Logaraj et al., 2000).

Fig 4 also highlights another very important element. All emulsions are bimodal and EIL_1.2_pH2.5 specifically is multimodal, a symptom of excellent stability as reported by (Mercado & Fuentes, 2017).

In Fig. 5, the emulsions at different pH, but at the same emulsification speed of 7600 rpm, are reported.

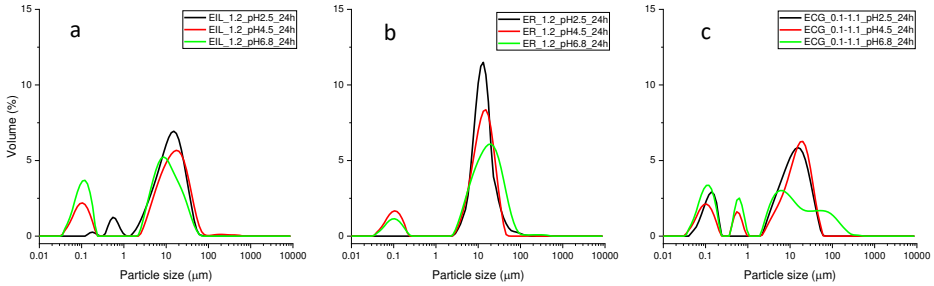

Fig.5: Particle size of C EIL_1.2_24h, ER_1.2_24h and ECG_0.1-1.1_24h at pH=2.5, 4.5 and 6.8.

By observing the different spectra in Fig.5, it is possible to note that pH affects the PSD and therefore particle distribution. In particular, the individual overlaps are analyzed. Looking the Fig.5a, as pH increases, the intermediate peak disappears and a marked increase in the first peak is evident, between 0.04 and 0.2 microns; the emulsion changes from multimodal to bimodal. As found by Mikulcová et al. (2018), the size distribution of droplets of emulsions prepared at pH 2.5 showed prevailingly the presence of large droplets. As seen for interfacial tension, chapter 2 sec. 3.1, at high CTAC concentrations and low pH there was a slight increase in IFT compared to pH 4.5 and 6.8, and this may be attributed to the fact that a more acidic environment excites the surfactant capacity of the endogenous bitumen molecules more, creating a competitive effect (Zhang et al., 2018).

The overlap of ER_1.2 spectra in Fig.5b shows a variation in the spike with decreasing pH. In particular, the sample ER_1.2pH2.5 has only a peak between 2 and 100 µm and when the pH increases this peak lowers and a second peak appears between 0.03 and 0.3 µm. In this case, because of the increment in the width of the curve, the coalescence phenomenon happens, where particles combine and grow larger, compromising stability (Mercado & Fuentes, 2017).

Finally, it is possible to observe the behaviour of the ECG_0.1-1.1 emulsion (Fig.5c). Comparing these spectra with that of CTAC, it is possible to observe that Guar causes some modification as pH varies. In particular, at pH=4.5, the emulsion changes from bimodal to multi-modal, increasing packing and thus also optimising its stability. This is no longer valid at pH=6.8, because the largest size peak becomes too large, reaching over 500 microns and thus losing stability. The limited emulsifying capacity of some biopolymers can be attributed to poor solubility and/or insufficient amphiphilic character to produce a rapid and substantial

lowering of the interfacial tension during droplet break-up, compounded by an unfavourable pH (Dickinson, 2003).

To confirm the results obtained from the DSD at 24 h as a function of pH, in Fig.6. the trend of the $d_{4.3}$ for all emulsions at the three pHs analyzed is reported from 24 h to 30 days.

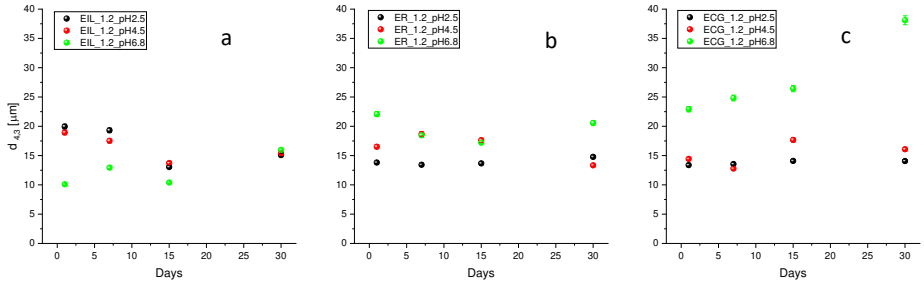

Fig.6: Evolution of $d_{4.3}$ over the time of EIL_1.2_24h, ER_1.2_24h and ECG_0.1-1.1_24h at pH=2.5, 4.5 and 6.8.

As can be seen in Fig.6, the trend of $d_{4.3}$ over time confirms the particle distribution. In Fig.6 a, it is evident that EIL_1.2_pH2.5 has the highest $d_{4.3}$ at 24 h, followed by the other two pH values- Since $d_{4.3}$, volume-weighted mean diameter is proportional to particle width (James, 2006), this result confirms what found from the particle distribution in Fig.5 a, where pH 2.5 has the largest peak size compared to pH 4.5 and 6.8, and one more intermediate peak than these, while pH 4.5 and 6.8 peaks appear with a smaller size.

With regard to Fig.6b, it is possible to see that as the pH increases, there is an increase in $d_{4.3}$, hence there is a presence of larger particles that is correlated to a lower stability (James, 2006).

Finally, the trend of $d_{4.3}$ for sample ECG_0.1-1.1 (Fig.6c) shows poor stability at pH=6.8, in contrast to pH=2.5 and 4.5, which shows a very similar $d_{4.3}$ trend, especially up to 15 days.

This could be attributed to the not excellent surfactant power of guar, a biopolymer, which may be disadvantaged by a nearly neutral pH com pH 6.8. The limited emulsifying capacity of some biopolymers can be attributed to poor solubility and/or insufficient amphiphilic character to produce rapid and substantial lowering of interfacial tension during droplet breakup. So, the large molecular mass of a typical hydrocolloid and a pH that is not favourable to the right dispersion, makes it an unlikely candidate for an ingredient with the highest emulsifying capacity (Dickinson, 2003).

Finally, to understand which laboratory production was the best, several overlays of the spectra were made, arriving at the one shown in Fig.7.

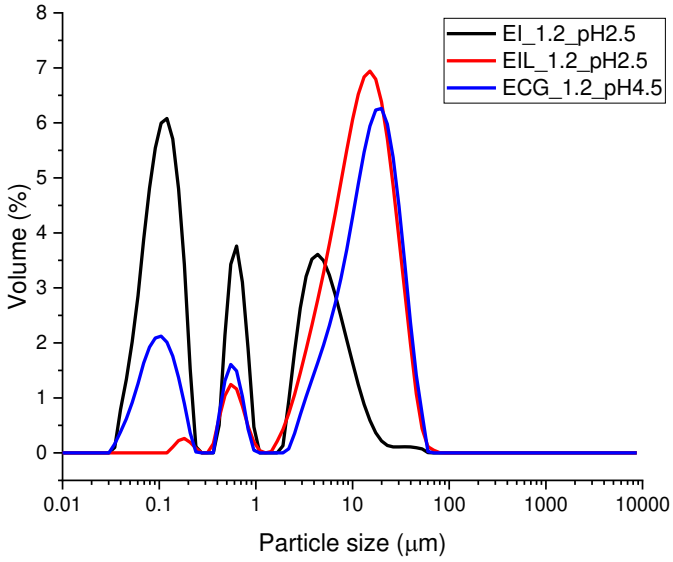

Fig.7: Overlay of particles distribution of EI_1.2_pH2.5, EIL_1.2_pH2.5 and ECG_1.2_pH4.5

Based on the above observations, the overlay of the most similar emulsions as particle distribution is shown in Fig.7

EIL_1.2_pH2.5 and ECG_1.2_pH4.5 are the most like industrial (EI), being the only ones characterized by three peaks. Both have the main particle peak shifted further to the right than that of EI, reaching particles of 100 microns: however, this was to be expected and is normal because it is related to the different emulsification tools, industrial colloid mill vs. ultra-turrax.

On the other hand, the intermediate peak, between 0.3-1 μm, is present for both, although a little less pronounced.

Finally, the peak of the smallest particles, below 0.1 μm, is only hinted at for EIL_1.2_pH2.5, while it is well evident and has a vertex just in 0.1 micron, as for EI, that of ECG_1.2_pH4.5.

From the overlay of Fig.7, which confirms previous comments, it is evident that the best reproduction is ECG_1.2_pH4.5, which contains guar as co-emulsifier, confirming that this greener formulation can still maintain microscopic features of the desired industrial standard.

3.2 Rheological measurements

The analysis of the viscosity was interesting and essential to confirm the PSD results.

Sample EIL_1.2_pH2.5 was analysed only at two 7600 and 10000 rpm because 10000 and 5200 appear similar by PSD.

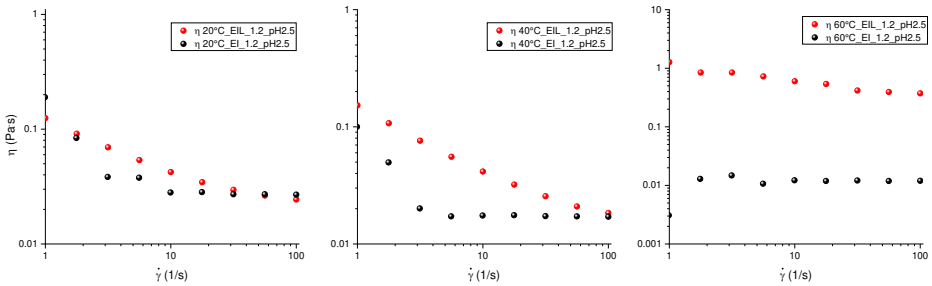

Fig. 8: Viscosity vs shear rate of EIL_1.2_pH2.5 emulsion at 10000 rpm and EI_1.2_pH2.5.

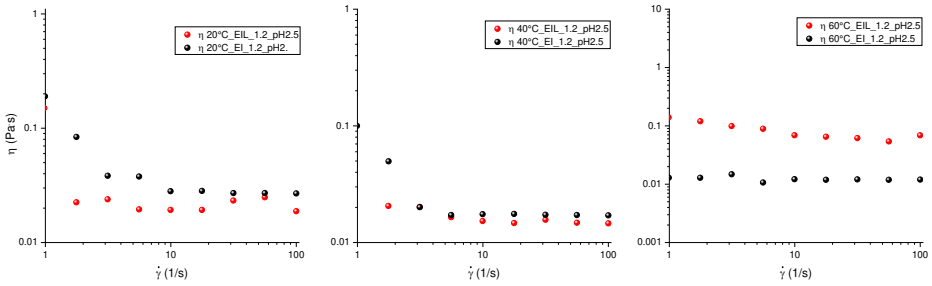

Fig. 9: Viscosity vs shear rate of EIL_1.2_pH2.5 emulsion at 7600 rpm and EI_1.2_pH2.5.

In Fig. 8 the viscosity of EIL_1.2_pH2.5 as a function of shear rate shows a shear thinning, beginning closer to the industrial emulsion viscosity.

Silva et al. (Silva et al., 2016) reported that, following the addition of substances to CTAC solutions, increasing pH leads to a progressive decrease in viscosity, while higher viscosities occur at lower pHs. This is related to the nature of the interactions between CTAC and the phase it is in, and the degree of ionization of the functional groups present in the latter, which are strongly dependent on temperature, which by increasing evidently favours the creation of new bonds/groups that consequently increase viscosity (Silva et al., 2016).

Since for industrial emulsion, this does not occur, The chosen emulsification method likely plays a crucial role in how strongly this phenomenon affects CTAC. In the colloidal mill, as also reported by the PSD in Fig.1, the particle distribution is so small that it is probably not affected by this phenomenon as is the case with laboratory reproduction, where the particle size is evidently larger, Fig.5a.

Fig. 9 shows the viscosity of EIL_1.2_pH2.5 which has a Newtonian behavior, like the industrial sample, and a low viscosity which allows excellent workability.

It is clear from Figs.8 and 9 that the different emulsification speeds influence the viscosity. In particular, the viscosity is lower at 7600 rpm, and this result confirms that the multimodal emulsion has a lower viscosity attributed to the packing of the emulsion droplets (Querol et al., 2017)

After choosing the best emulsification speed, all the emulsions shown in Tab.1 were rheological characterized.

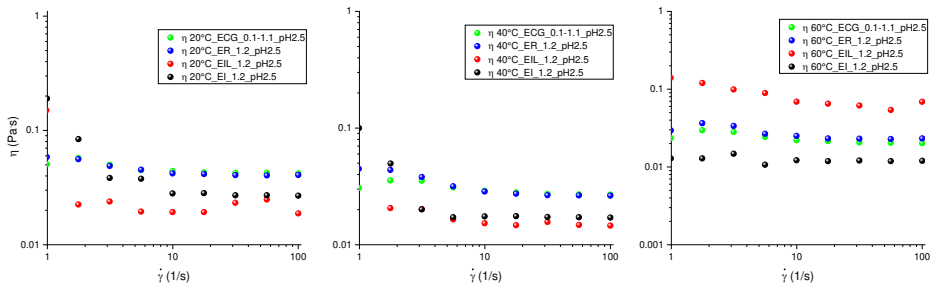

Fig. 10: η vs shear rate of all emulsions at 7600 rpm at T=20°, 40° and 60°C.

The viscosity trends are reported in Fig.10. The viscosities of ER_1.2_pH2.5 and ECG_1.2_pH2.5 show a Newtonian behavior and are also in the same order of magnitude for all the temperatures analyzed.

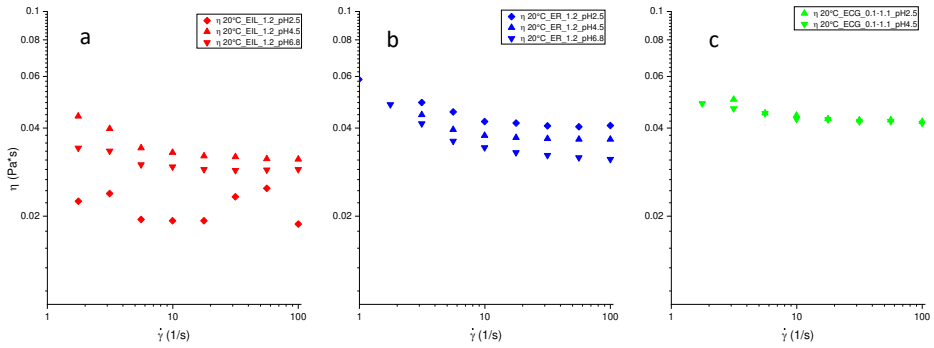

Fig. 11: η vs shear rate of all emulsions at pH=2.5, 4.5 e 6.8 at T=20° C.

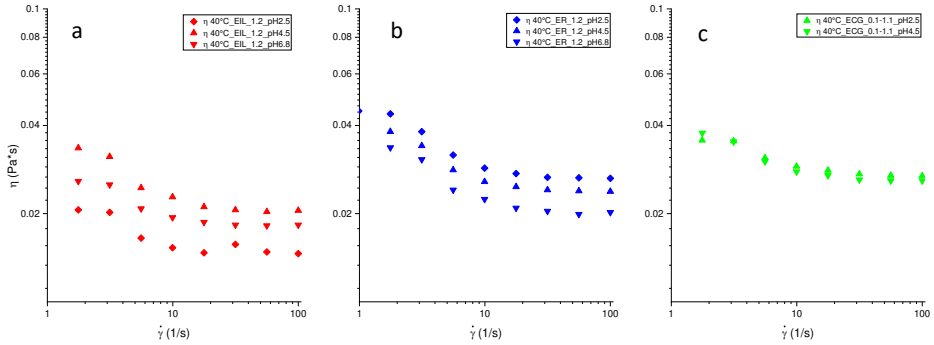

Fig. 12: η vs shear rate of all emulsions at pH=2.5, 4.5 e 6.8 at T=40°C

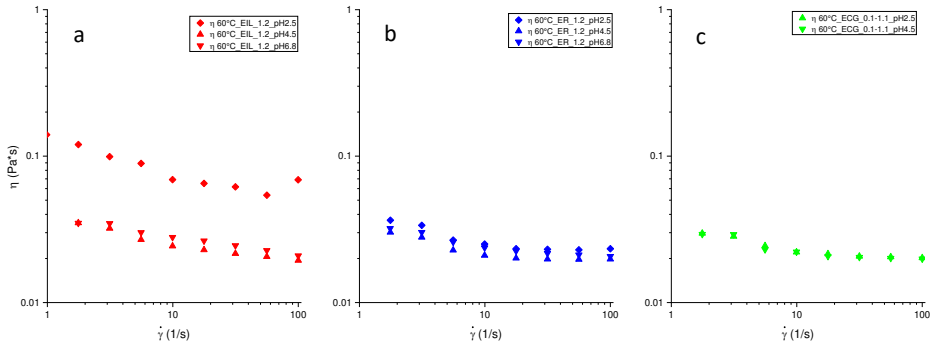

Fig. 13: η vs shear rate of all emulsions at pH=2.5, 4.5 e 6.8 at T=60°C

Looking at the bulk of EIL_1.2, Fig.11a, 12a and 13a, it is immediately clear that as pH increases from 2.5 to 4.5 and 6.8, there is an increase in viscosity for 20° and 40°C. This result is reflected in the PSD shown in Fig. 5a. The spectrum at pH 4.5 and 6.8 is characterized by the presence of two peaks. The spectrum at pH 2.5, on the other hand, is characterized by three peaks that evidently allow for better packing and, therefore, a decrease in viscosity (Querol et al., 2017).

The only temperature at which there is a reverse is T=60°C, viscosity decreases at pH=4.5 and 6.8, increasing at pH=2.5. This increase is most likely due to the interaction of CTAC with something that is favoured by a more acidic environment and high temperatures. As reported by Silva et al., for a neat solution of CTAC, as pH increases shear viscosity increases, but they also reported that the addition of substances to the CTAC solution reverses the situation and increasing the pH mixtures leads to a progressive decrease in the shear rate viscosities (Silva et al., 2016).

This result is related to the nature of the interactions between CTAC and the substance added, and to the ionization degree of the functional groups present in the chemical structure of this substance, which are obviously also influenced by temperature.

The phenomenon described by Silva et al. could explain what happens to the system studied in this paper: when the soap solution containing the CTAC enters the extremely complex bituminous system, where substances interacting with the surfactant are present, especially at low pH and high temperatures, behaviors similar to those found in the literature occur.

Particle distribution, in Fig.5a, showed the disappearance of the second peak at pH = 2.5 and the increase of a smaller size peak as pH increases. Consequently, the lower packing and the increase of one particle size class could fully justify the slight increase in viscosity found in Fig.s.11a and 12a.

In the case of Redicote, however, η decreases at all temperatures as pH increases, as shown in Fig.11b, 12b and 13b. This viscosity behaviour is associated with an increase in instability, as confirmed by PSD in Fig.5b, which causes particle precipitation and coalescence (Mercado & Fuentes, 2017).

Finally, the overlay for ECG_0.1-1.1 was only carried out for pH=2.5 and 4.5 because PSD has shown that the spectrum at pH=6.8 was too far off.

The emulsion ECG_0.1-1-1_pH=6.8 exhibited visible separation and was therefore excluded from further analysis. This aligns with the ζ-potential measurements of the CTAC-containing emulsion in Section 3.3, Chapter 2. Since CTAC is the primary surfactant in ECG_0.1-1-1, only emulsions at pH 2.5 were monitored in cylinders. Higher pH values were deemed unsuitable due to instability below the minimum stability threshold. To confirm this, following the PSD in Fig.5, monitored the emulsion ECG_0.1-1-1_pH=6.8, the separation was clear: water at the surface and lumpy pulp at the bottom. For all the other emulsions analyzed at 24h, a light mechanical stirring was sufficient to obtain another time the emulsion back as for the industrial emulsion.

This is most likely because, even if modified, the guar-gum has more stabilizing properties than surfactant and the near-neutral pH emphasizes its low surfactant character even less (Dickinson, 2003).

Figs. 11c, 12c, and 13c show that the viscosity does not change for the two pHs under analysis, further confirming that for this formulation, the use of a higher pH, and thus less acid use in favour of greater sustainability, does not affect viscosity.

PSD analysis shown in Fig.5c, shows the appearance of another peak at pH=4.5 for the system, with the combination of CTAC and GUAR. This pH effect is indicative of stability because the emulsion changes from bimodal to trimodal resulting from increased packing (Mikulcová et al., 2018; Querol et al., 2017) and is confirmed by an unchanged bulk.

In light of the above, the system obtained, less acid and with a lower quantity of CTAC, could be used for soap solutions, resulting in an alternative to the industrial emulsion at pH 2.5

Bibliography

Cardona, D. A. R., Pouget, S., Di Benedetto, H., & Olard, F. (2015). Viscoelastic behaviour characterization of a gap-graded asphalt mixture with SBS polymer modified bitumen. Materials Research, 18(2), 373–381. https://doi.org/10.1590/1516-1439.332214

Dickinson, E. (2003). Hydrocolloids at interfaces and the influence on the properties of dispersed systems. Food Hydrocolloids, 17(1), 25–39. https://doi.org/https://doi.org/10.1016/S0268-005X(01)00120-5

James, Alan. (2006). Overview of asphalt emulsion. Transportation Research Circular, August, 1–15.

James, Alan., Yuliestyan, A., Cuadri, A. A., García-Morales, M., Partal, P., Lévenard, F., Gaudefroy, V., Petiteau, C., Chailleux, E., Capron, I., Bujoli, B., Ramli, N; Mohd Sobani, S. S. ;, SCOTT, J. A. N., Silva, K. N., Novoa-Carballal, R., Drechsler, M., Müller, A. J. A. H. E., Penott-Chang, E. K., Müller, A. J. A. H. E., … Partal, P. (2017). Overview of asphalt emulsion. Colloids and Surfaces A: Physicochemical and Engineering Aspects, 14(February), 242–251. https://doi.org/10.1016/j.jcis.2010.09.059

Klink, I. M., Phillips, R. J., & Dungan, S. R. (2011). Effect of emulsion drop-size distribution upon coalescence in simple shear flow: A population balance study. Journal of Colloid and Interface Science, 353(2), 467–475. https://doi.org/10.1016/j.jcis.2010.09.059

Logaraj, S., Ernzen, T., Lin, M., Hays, T., & Stegemoeller, C. (2000). Emulsification A solution to Asphaltene Handling Problems. ISSA/AEMA 2nd Joint Conference, 12.

Mercado, R., & Fuentes, L. (2017). Measure of asphalt emulsions stability by oscillatory rheology. Construction and Building Materials, 155, 838–845. https://doi.org/10.1016/j.conbuildmat.2017.08.095

Mikulcová, V., Bordes, R., Minařík, A., & Kašpárková, V. (2018). Pickering oil-in-water emulsions stabilized by carboxylated cellulose nanocrystals – Effect of the pH. Food Hydrocolloids, 80, 60–67. https://doi.org/10.1016/j.foodhyd.2018.01.034

Querol, N., Barreneche, C., & Cabeza, L. F. (2017). Method for controlling mean droplet size in the manufacture of phase inversion bituminous emulsions. Colloids and Surfaces

A: Physicochemical and Engineering Aspects, 527(May), 49–54. https://doi.org/10.1016/j.colsurfa.2017.05.018

Querol, N., Barreneche, C., & Cabeza, L. F. (2019). Asphalt emulsion formulation: State of the art of formulation, properties and results of HIPR emulsions. Construction and Building Materials, 212, 19–26. https://doi.org/10.1016/j.conbuildmat.2019.03.301

Silva, K. N., Novoa-Carballal, R., Drechsler, M., Müller, A. H. E., Penott-Chang, E. K., & Müller, A. J. (2016). The influence of concentration and pH on the structure and rheology of cationic surfactant/hydrotrope structured fluids. Colloids and Surfaces A: Physicochemical and Engineering Aspects, 489, 311–321. https://doi.org/10.1016/j.colsurfa.2015.10.054

Yuliestyan, A., Cuadri, A. A., García-Morales, M., & Partal, P. (2016). Binder Design for Asphalt Mixes with Reduced Temperature: EVA Modified Bitumen and its Emulsions. Transportation Research Procedia, 14, 3512–3518. https://doi.org/10.1016/j.trpro.2016.05.319

Yuliestyan, A., García-Morales, M., Moreno, E., Carrera, V., & Partal, P. (2017). Assessment of modified lignin cationic emulsifier for bitumen emulsions used in road paving. Materials and Design, 131(February), 242–251. https://doi.org/10.1016/j.matdes.2017.06.024

Zhang, S., Zhang, L., Lu, X., Shi, C., Tang, T., Wang, X., Huang, Q., & Zeng, H. (2018). Adsorption kinetics of asphaltenes at oil/water interface: Effects of concentration and temperature. Fuel, 212(September 2017), 387–394. https://doi.org/10.1016/j.fuel.2017.10.051

Chapter 4

1. Introduction

This chapter focuses on the emulsion breakdown and the rheological properties of them. The properties that characterize pavements made with bitumen emulsions are given, principally, by the residual bitumen following emulsion breakdown. Cold bitumen emulsion mixtures (CBEM) utilize water instead of heat. This reduces the viscosity of the bitumen, enabling it to be mixed with cold and wet aggregates at ambient temperatures (Garilli et al., 2019a).

Compared to hot mixtures, CBEM offers several advantages. It significantly reduces energy consumption, leading to a lower environmental impact (Goyer et al., 2012). In addition to its environmental benefits, pavement recycling technologies provide cheaper, faster, and less traffic disruptions alternative to conventional reconstruction strategies (Alkins et al., 2008).CBEM technology goes beyond just mixing. By lowering both paving and service temperatures, it significantly reduces toxic emissions, safeguarding the environment, and workers' health, and delivering a double win for both the economy and the environment.

When the water and bitumen particles are separated and the latter is merged again, producing a bituminous film, the emulsion is broken and it is largely used for surface treatment, such as slurry surfacing, reinstatement work on low trafficked, walkways, tack coating and cold recycling (Raposeiras, 2013). Several materials are used to promote the breaking emulsions, including waste products, polymers, and fibers of various kinds, but certainly, the most widely used nowadays is cement (Garilli et al., 2019b)

The breaking process in bituminous emulsions is complex and involves several proposed mechanisms. One such mechanism is the adsorption of emulsifiers onto the surface of mineral aggregates. This can disrupt the stability of the emulsion and promote the coalescence of bitumen droplets. Another factor is thought to be a rise in pH, which can neutralize the charge on the emulsifier and destabilize the emulsion. Additionally, the release of ionic species from the aggregates or the environment can also influence breaking (Boucard et al., 2015). To cater to diverse applications, bituminous emulsions are formulated with different breaking rates. Fast-breaking emulsions are ideal for tack coats, where a rapid formation of a strong bond between the new layer and the existing pavement is desired (Albayati et al., 2018).

While CBEM offers significant environmental and economic benefits, its mechanical properties are not as robust and effective as those of hot mix asphalt (Serfass et al., 2012). As said before, cement is generally added to break the emulsions and it seems that it also improves the mechanical properties of CBEM (Garilli et al., 2019a). Even at small dosages (less than 1% by mass of dry aggregate), cement has important effects on the emulsion breaking and setting process and can improve the short-term performance of cold mixtures by increasing their stiffness, and moisture resistance (Z. Wang & Sha, 2010). Increasing the cement content in the mixture beyond 2% by weight (w/w) promotes the formation of a cementitious structure, leading the mixture to behave more like cemented (Fang et al., 2016). This is because the overall performance, including strength and stiffness, is influenced by the balance between the residual bitumen from the emulsion and the cement content. This ratio is referred to as the bitumen/cement ratio (B/C).

A distinctive feature of CBEM is that their physical and mechanical properties evolve because emulsion breaking and setting, moisture loss and hydration of cement are all time-dependent processes (Cardone et al., 2015). The study of this process, known as curing, is of the utmost practical importance because freshly mixed CBEM should be plastic and workable to allow laydown and compaction, whereas after construction the development of internal cohesion and suitable mechanical properties should be as fast as possible to allow construction of the upper layers and opening to traffic (Graziani et al., 2016).

Two main causes for bitumen emulsion breaking in contact with mineral aggregates were described by Lesueur and Potti (Leuseur 2014): the increase of bitumen droplet concentration and the disappearance of electrostatic repulsion between bitumen droplets. Cement addition in CBEM influences both destabilization mechanisms. Firstly, cement hydration reduces free water in the mixture (Fang et al., 2016), , promoting bitumen droplet coalescence. Secondly, it increases pH, potentially neutralizing the stabilizing effect of cationic emulsifiers (F. Wang et al., 2013). In this regard, over-stabilized emulsions are specifically formulated to allow the mixing of high cement dosages avoiding premature breaking. On the other hand, both cationic and anionic emulsifiers may have a retarding effect on cement hydration at an early age (i.e. cement setting) and also cause a loss in the long-term content of cement hydrates (Tan et al., 2014).

However, the cement asphalt emulsion composite (CAEC) stability is greatly challenged during the preparation process due to the inherent properties of CAEC. The traditional

Derjaguin-Lan dau-Verwey-Overbeek (DLVO) theory indicates that any factor that changes the electric potential between the particles in the emulsion can affect the stability of the emulsion (Lei et al., 2020). The release of mineral ions by cement hydration and the resulting change in pH value of the solution can affect the surface potential of particles, the water absorption characteristics of cement particles during the hydration process and the imbalance of temperature caused by the exothermic heat of cement hydration (Rutherford et al., 2014)can jointly change the stability of the asphalt emulsion. The process of flocculation, coalescence and formation of asphalt film developed by the AE particles in an unstable state can interact with the change of surface potential (Rutherford et al., 2014) and the increase of cement particle size, which can cause the CAEC mortar's work performance to violently oscillate (Tan et al., 2014). Then the distribution of heterogeneous media in hardened composites, as well as the phase geometry and macroscopic mechanical properties can be affected (Miljković et al., 2017).

Because of the strong time-dependency of the curing process and the need to significantly improve properties, large amounts of cement must sometimes be added, resulting in excessive stiffness and poorly elastic and deformable pavements, others have tried to replace cement with waste materials and cylinders oil with fair results (Borhan et al., 2007; Thanaya, 2003).

Recognizing that the properties of residual bitumen from emulsion play a crucial role, this chapter focuses on analyzing the impact of different surfactants on the final characteristics of the bitumen film. On the emulsions produced, the percentage of residual solids was first checked.

Following, according to a European green standard on emulsion drying as a simulation of breakage (NORMATIVA EN 13074-1:2011 e EN 13074-2:2011), the recovered bitumen was subjected to penetration, ring and ball softening temperature tests, and rheological analyses. The viscoelastic master curves are generated using the least squares Levenberg–Marquardt (L–M) method based on the time-temperature superposition principle (Yin et al., 2018)

An asphalt pavement not only endures a rapid traffic load but is also subjected to the temperature-stress relaxation and creep deformation of the steep-slope surface layer, caused by the long-term load experienced for tens of hours or even decades. However, it is not possible to perform in a laboratory using the current technology, because it is difficult to

grasp the law of materials over such a wide range of temperatures and loading time. The time-temperature superposition (TTS) principle can analyze the viscoelastic properties of asphalt pavement materials in a wide range of temperatures and loading times (Huang et al., 2018). The master curves of viscoelastic materials can predict their mechanical properties at various temperatures and frequencies or loading time can yield the physical properties completely by using the constitutive model.

The tests above mentioned are performed only on the best-performing emulsions prepared in chapters 2 and 3 because it is assumed that pH does not affect the recovered bitumen. Therefore, bitumen was recovered from the emulsions at pH=2.5, to have the comparison with the industrial one (EI), and only ECG_1.1-0-1 was also recovered from the emulsion at pH=4.5, because it is very high-performing, to understand if there is a difference or not.

After having developed the recovery technique, the use of a fiber obtained from citrus fruit waste as a replacement for cement for breaking was tested on the industrial emulsion (EI). The replacement of cement in favour of natural fiber was decided to improve the performance of the road pavement in terms of rigidity and flexibility. Initially, the fiber was replaced following the standard used for breaking with cement, subsequently, the procedure was modified to improve the process.

The results were satisfactory, both in terms of the final properties of the emulsion/fiber mix and in terms of the rheological properties of the final residue obtained.

2. Materials and Methods

2.1 Materials

An industrial emulsion (EI), kindly provided by Valli Zabban S.r.l. (Italy), was used as a reference in this study. REDICOTE E11, provided by Nouryon (Sweden), Guar-Gam Esaflor (Marchemical Lab. S.r.l (Italy)) and Cetyltrimethylammonium Chloride (CTAC, M.W. = 320 g/mol), were used as emulsifiers to realize laboratory emulsions.

A virgin bitumen with penetration grade 50/70, was kindly supplied by Valli Zabban S.r.l (Italy) and used for all the emulsions and investigations.

Distillate water and chloridric acid (37% w/w) (Titolchimica, Italy), were used to prepare emulsions.

A Citrus fiber (Aglufibers) was kindly provided by JRS Silvateam Ingredients (Italy) and used for breaking emulsions. It is hydrophilic and with partial negative charge.

2.2 Bituminous emulsions

The emulsions were prepared as described in Chapter 2, Section 2.3. The samples analyzed were reported in Table 1.

ID	**Surfactant type**	**Guar % (w/w)**	**CTAC % (w/w)**	**Redicote E11 % (w/w)**
ECG_0.1-1.1_pH2.5	CTAC-GUAR	0.1	1.1	0
ECG_0.1-1.1_pH4.5	CTAC-GUAR	0.1	1.1	0
ECG_0.1-1.1_pH6.8	CTAC-GUAR	0.1	1.1	0
ER_1.2_pH2.5	REDICOTE E11	0	0	1.2
ER_1.2_pH4.5	REDICOTE E11	0	0	1.2
ER_1.2_pH6.8	REDICOTE E11	0	0	1.2
EI_1.2_pH2.5	CTAC	0	1.2	0
EIL_1.2_pH2.5	CTAC	0	1.2	0
EIL_1.2_pH4.5	CTAC	0	1.2	0
EIL_1.2_pH6.8	CTAC	0	1.2	0

Tab.1: ID emulsions analyzed.

2.3 Samples fiber-addition

The samples analyzed with fiber addition are shown in Tab.2

ID	**Emulsion**	**Fiber suspension (g_{fiber}/150 $g_{Distillate-water}$)**
EI_5FS	EI_1.2_pH2.5	5/150
EI_7.5FS	EI_1.2_pH2.5	7.5/150
EI_10FS	EI_1.2_pH2.5	10/150

Tab.2: ID fiber-added emulsions.

The fibers were dispersed in distilled water and then the suspension was added to 100 grams of industrial emulsion.

2.4 Residual bitumen

The residual bitumen of emulsions shown in Tab.3 was analyzed.

ID	**Surfactant type**	**Guar** % **(w/w)**	**CTAC** % **(w/w)**	**Redicote E11** % **(w/w)**
RB_ECG_0.1-1.1_pH2.5	CTAC-GUAR	0.1	1.1	0
RB_ECG_0.1-1.1_pH4.5	CTAC-GUAR	0.1	1.1	0
RB_ER_1.2_pH2.5	REDICOTE E11	0	0	1.2
RB_EI_1.2_pH2.5	CTAC	0	1.2	0
RB_EIL_1.2_pH2.5	CTAC	1.2	0	0

Tab.3: ID recovered bitumen of emulsions.

Table 4 shows the bitumen samples ID recovered from the fiber-added emulsions.

ID	**Emulsion**	**Fiber suspension** ($\mathbf{gr_{fiber}/150gr_{Distillate\text{-}water}}$)
RB_EI_5FS	EI_1.2_pH2.5	5/150
RB_EI_7.5FS	EI_1.2_pH2.5	7.5/150
RB_EI_10FS	EI_1.2_pH2.5	10/150

Tab.4: ID recovered bitumen of fiber-added emulsions.

2.5 Methods

2.5.1 Percent of solids

The procedure employed to calculate the percentage of solids is as follows:

- an empty Petri dish is weighed and marked the weight (T);

- enough emulsion is poured to cover the Petri dish base and marked that weight (W_1);
- the Petri dish is conditioned in the oven for 24 hours at 70°C;
- following oven conditioning, the Petri dish is weighed again and the new weight is marked (W_2).

Equations 1 and 2 are used to calculate the solids percentage:

$$W_{emu}^{24\,h} = W_2 - T \qquad \text{Eq.1}$$

$$\%Solids = \frac{W1}{W2} \cdot 100 \qquad \text{Eq.2}$$

2.5.2 Emulsion breaking by fiber-addition

The fiber suspension was added to the industrial emulsion with the aim of breaking the emulsion. Two procedures were performed for the realization of the emulsion breaking, the first according to the standard procedure with cement (UNI EN 12848), and the second according to a procedure developed in the laboratory to disperse the fibers. Particularly speaking, the fiber in water was dispersed with Ultraturrax T50 (IKA-WERKE, Germany) equipped with G45F tool at 8000 rpm for 5 minutes and then added to 100 g of industrial emulsion by manual mixing

Three amounts of fiber were selected, 5, 7.5 and 10 g and added to 150 g of distilled water.

2.5.3 Recovered bitumen

The binder recovery procedure was performed according to EN 13074-1:2011 and EN 13074-2:2011 standards. 100 gr of emulsion were poured into a silicone mold having dimensions according to the standard. The mold was conditioned in an oven (BINDER, Germany) at 25°C for 24h, for another 24 h at 50°C and finally at 85°C for 24 h.

2.5.4 Penetration and ring and ball (R&B) softening temperature tests

The penetration test on bitumen is a measure of the hardness or consistency of bituminous material (Kalpana et al., 2020). This test is used for evaluating the consistency of bitumen and it was performed according to UNI EN 1426.

The softening point of bituminous material, instead, can be defined as the temperature at which this bituminous material further softens after its arbitrary softness point is reached (Kalpana et al., 2020). Ring and ball (R&B) softening temperature tests were determined according to UNI EN 1247.

2.5.5 Rheological analysis

Dynamic Shear Rheological (DSR) measurements on bituminous emulsion and recovered bitumen from these and fiber-added emulsions were carried out using a controlled shear stress rheometer (Haake Mars III, Thermo Fisher Scientific, Germany), and equipped with a Peltier system for temperature control.

A titanium parallel plate (P50 Ti L, Φ = 50mm, polished, gap=1 ± 0.1 mm) was used for bituminous emulsion, while for fiber-added emulsions and recovered bitumen from these was used a titanium parallel plate (P20 Ti L, Φ = 20mm, polished, gap=1 ± 0.1 mm).

The rheology of bitumen recovered from base emulsions, on the other hand, was obtained employing a controlled stress rheometer, MCR 702e (Anton Paar, Austria), equipped with parallel plate geometry of 25 mm or 8 mm (according to sample consistency for high and low temperatures), a measure gap of 2 ± 0.1 and a Peltier system for temperature control.

Flow curves in the range between 0.1 to 100 s^{-1} were carried out on the emulsions.

The recovered binder of the emulsion was rheologically analyzed according to European standards; in particular, frequency sweep tests at high temperature (T=40-100°C) and at low temperature (T=40-(-30)°C) were performed. To completely investigate the physical properties of the recovered binder, their viscoelastic master curves are generated using the least squares Levenberg–Marquardt (L–M) method based on the time-temperature superposition principle (Yin et al., 2018). In this study, the limit of obtaining the viscoelastic master curves of the five recovered bitumens using the Williams-Landel-Ferry (WLF) and Arrhenius equations is analyzed. Next, the recovered binder belonging to the category of

simple thermo-rheological materials is verified by conducting the dynamic frequency sweep test.

On the recovered bitumen from fiber-added emulsions, frequency sweep tests in the Linear viscoelastic region (LVR), previously determined by time and stress sweep tests at 20°, 40° and 60°C, were performed. Moreover, time cure tests between 20 and 80°C at a rate of 1°C/min were done.

Each measurement was at least twice and the mean value and standard variation were reported.

3. Results

3.1 Percentage of solids

The solids percentage was calculated according to Eq.1 and Eq.2 suggested in Sec.2.3.1 and the values were put in Table 5 below.

pH	%S EIL_1.2	%S ER_1.2	%S ECG_1.1-0.1
2.5	62.7 ± 0.02	65.7 ± 0.01	64.3 ± 0.03
4.5	63.2± 0.03	65.5 ± 0.01	63.4 ± 0.03
6.8	63.1 ± 0.01	64 ± 0.03	62 ± 0.02

Tab.5: Percentage of the solids of the emulsions analyzed.

As can be seen from Table 5, there is a small increase in the solids fraction in all emulsions, due to the evaporation and overheating phenomena of the emulsification.

In general, the percentage of solids for the EI_L _1.2% samples is constant with pH, ER_1.2% has the largest fraction of residual solids, and ECG_1.1-0.1% has a downward trend with pH.

In particular, the best emulsions in terms of solid percentage are EIL_1.2_pH2.5 and ECG_1.1-0.1_pH4.5 and 6.8. This confirms that similar to previous analyses, for the guar-

based emulsion ECG_1.1-0.1, an increase in pH favors a better result due to the guar-acid environment interaction (Dickinson, 2003).

3.2 Penetration and ring-ball temperatures

Table 6 reports the penetration and ring and ball results for all the samples analysed.

SAMPLE	**Penetration (mm/10)**	**T ring-ball (°C)**
EIL_1.2_pH2.5	30.6 0± 0.02	54.10 ± 0.04
ER_1.2_pH2.5	34.30 ±0.02	53.40 ± 0.05
ECG_1.1-0.1_pH2.5	40.30 ± 0.04	52.80 ± 0.02
ECG_1.1-0.1_pH4.5	42.30 ± 0.05	52.60 ± 0.03
EI_1.2_pH2.5	35.30 ±0.04	53.30 ± 0.04

Tab.6: Penetration and ring-ball temperatures of analyzed emulsions.

As can be seen in Table 6, the emulsions reproduced in the laboratory provided excellent results in terms of residual bitumen penetration and ring-ball temperature tests. In particular, the emulsions obtained with a small quantity of Guar, ECG_1.1-0.1_pH2.5/pH4.5, have a higher penetration value, which can be connected to a lower stiffness compared to the standard emulsions obtained also in the lab (EIL_1.2_pH2.5). It would be interesting to obtain these emulsions under the same conditions as the industrial emulsion to be able to compare their properties. It is possible that guar, a biopolymer with a viscous nature, can provide a higher degree of elasticity to the system, which then decreases the stiffness (Marek Iwański 2011.Pdf, n.d.), allowing to obtain better-performing residual bitumen in the characteristics when analyzed with these tests. As concerns the ring and ball temperature, there are no evident trends with the emulsifier type or pH. At least a variation of about 1°C is observable.

3.3 Rheological measurements

3.3.1 Recovered bitumen from emulsion

The rheological characterization of the binder recovered from the bituminous emulsions is reported in this section.

Some studies have shown that the temperature and loading time effects on the mechanical relaxation process of viscoelastic materials are equivalent (Chailleux et al., 2006) Specifically, the mechanical properties of viscoelastic materials at a low temperature are equivalent to those obtained with a short loading time (or higher strain rate and higher frequency) based on the time-temperature equivalence principle, TTS.

The viscoelastic master curves generated by the least squares L–M method, as described in section 2.4.5, are in good agreement at moderate and high temperatures, as shown in Fig.1.

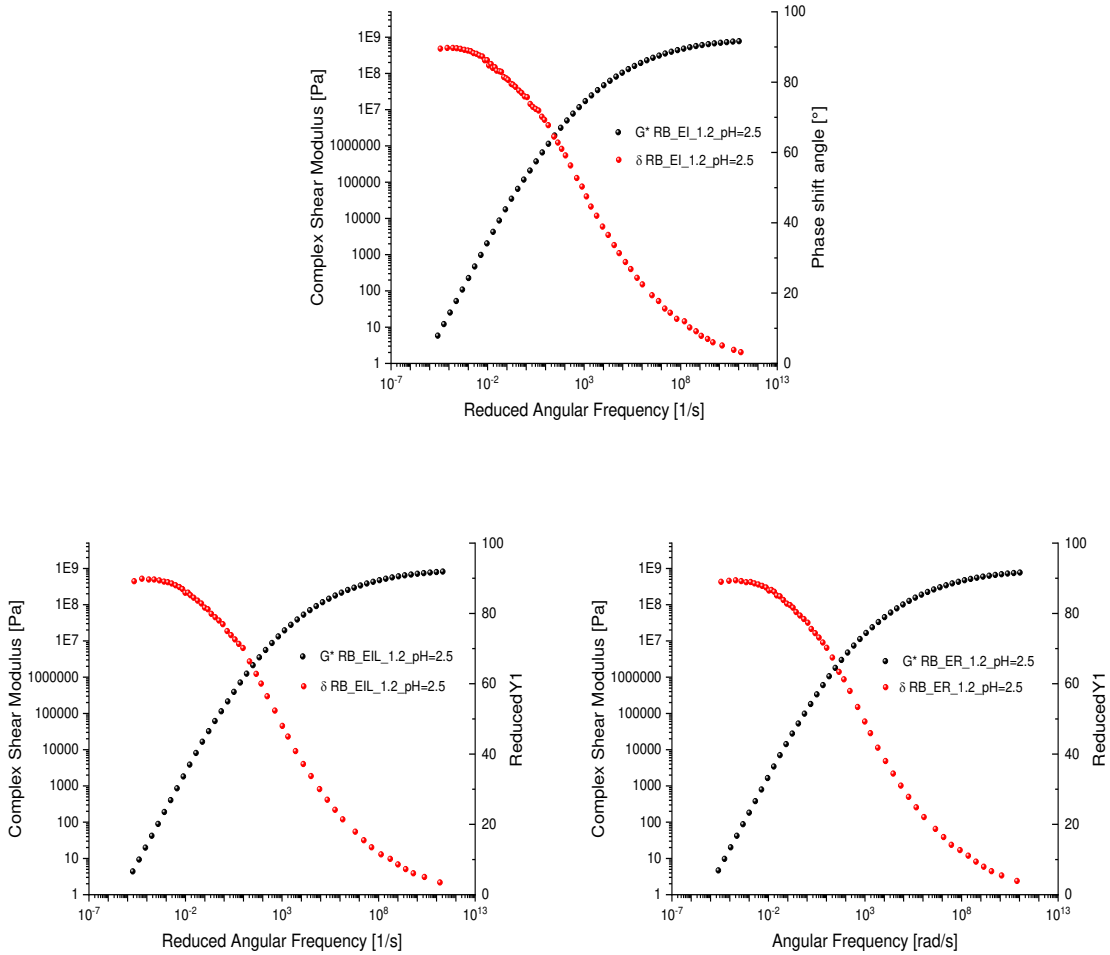

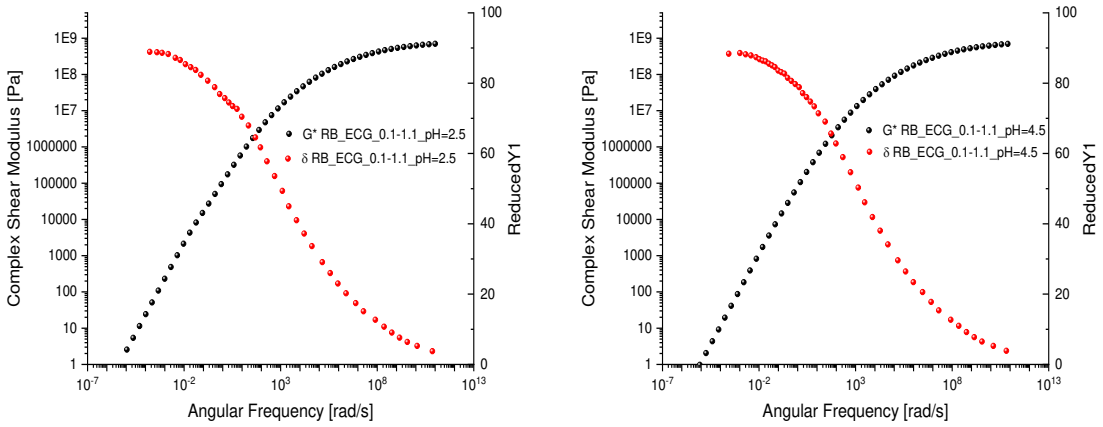

Fig.1: Mastercurves of recovered bitumen from industrial and laboratory emulsions.

Figure 1 shows the master curves of the recovered binder from laboratory emulsions and industrial one at 40 °C obtained by the L-M method. The superposition obtained by the L-M method at all frequencies is equivalent to the temperatures for the TTS principle. A horizontal shift factor was applied.

The L-M method proves to be a reasonable and feasible approach for constructing master curves of asphalts and asphalt mixtures. Small and possible deviations observed at specific data points could be related to the glass transition temperature (Tg) of the recovered bitumen (Yin et al., 2018), which can vary slightly depending on the surfactant chemistry.

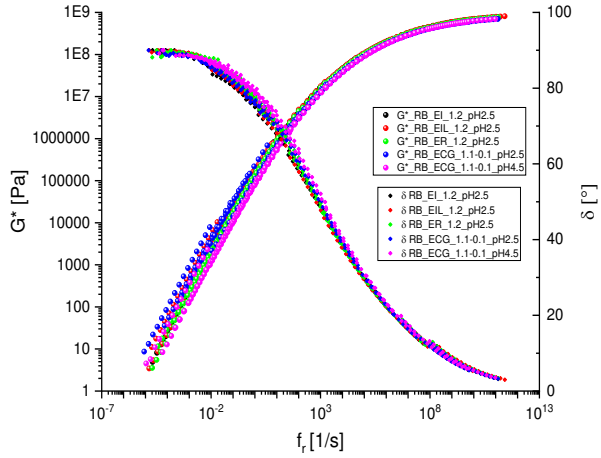

Fig.2: Overlay Mastercurves of recovered bitumen from emulsions.

Based on Figure 2, it can be concluded that the various surfactants employed minimally affect the recovered bitumen. They do not alter its rheological properties.

3.3.2 Fiber-added emulsions

The effect of the fiber addition to the emulsion, used as a substitute for cement for breaking, was analyzed rheologically according to the "*material and method section*".

To understand how fiber addition affects the emulsion and characterizes the fiber paste, flow curve analyses were performed on the three fiber-added emulsions and the virgin emulsion.

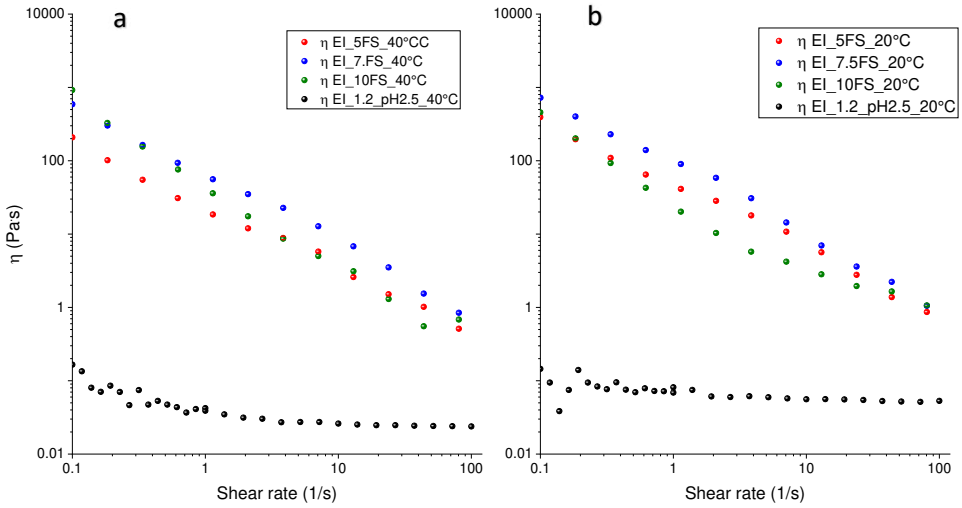

Fig.3: Flow curves for samples EI_FS at 20 (b) and 40°C (a) with the addition of three different percentages of fiber, compared to the virgin emulsion.

Figures 3 (a) and (b) show the influence of the fiber addition on the viscosity in the shear rate range between 0.1 to 100 s^{-1} compared with the net industrial emulsion (EI). All fiber-added emulsions show shear thinning behaviour, while the net bituminous emulsion is Newtonian. It is evident that the fiber addition has a marked influence on the viscosity of the bituminous emulsion structuring it. Although small amounts of fiber were added to the emulsion, the viscosity increased by up to three orders of magnitude as it occurs after the addition of cement, as reported by Xing Fang et al in the literature after the addition of cement. The cement showed a markedly different influence on the viscosity and mechanical properties of bitumen emulsion/cement blends. When the mass of added cement is less than 6% (corresponding to volume fractions lower than 0.02), adding cement makes the blends

more elastic and less shear-thinning, while at higher concentrations also the viscosity at low shear rates is dramatically increased (Fang et al., 2016).

The viscous property of cement emulsion asphalt was conferred by the addition of the asphalt component and cement in the material. However, compared with asphalt binders and mixtures (Shu & Huang, 2008), cement emulsion asphalt exhibits a higher viscosity. This is due to asphalt binders acting as a matrix in asphalt mixtures and binds fine and coarse aggregate particles together, while CEA, the asphalt components were incorporated into the cement paste matrix and the cement matrix and bound by the matrix itself (Rutherford et al., 2014). The viscous effect of the asphalt was significantly reduced by the cement paste and this is apparently what happens with the fiber (Fig.3), which creates a network that contains the base bitumen and increases its viscosity.

Given the consistency of the fiber paste, it was decided to perform also oscillatory tests on these samples to find out their frequency response.

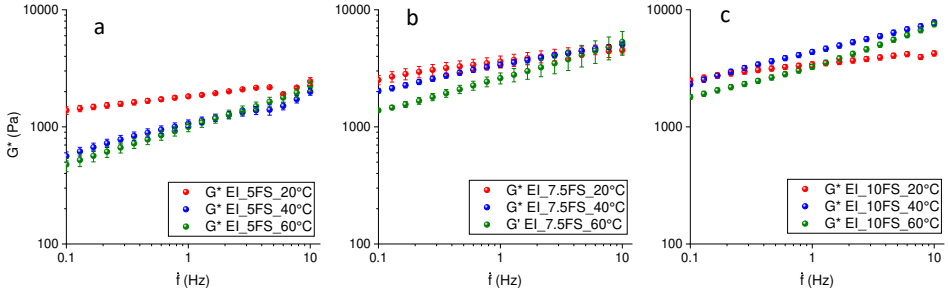

Fig.4: Frequency sweep tests for samples EI_FS at 20, 40 and 60°C with the addition of three different percentages of fiber, respectively (a), (b) and (c) compared to the virgin emulsion.

All the modified emulsions show a frequency-dependent behaviour that is influenced by the temperature. The sample with the lower quantity of fiber added shows a complex modulus lower than the other samples. Only at 20°C it is possible to observe a strong gel behaviour with low or dependence from the frequency.

As reported by Tyler Rutherford et al. (Rutherford et al., 2014), the dynamic modulus of CEA (cement emulsion asphalt) increased with the increase in loading frequency. On the other hand, as temperature increased, the dynamic modulus decreased and the fiber addition would appear to behave similarly to cement.

The temperature behavior was also investigated and the results are reported in Figures 5 (a) and (b).

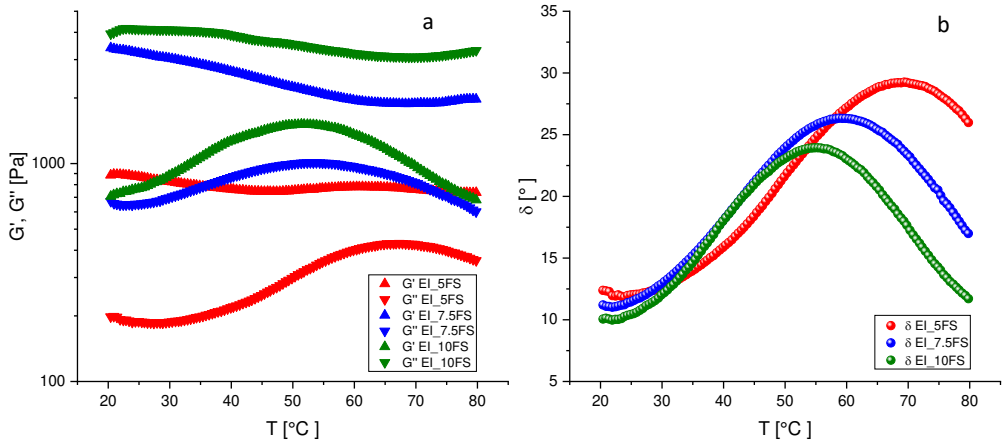

Fig.5: Overlay Time cure test test of EI_5FS, EI_7.5FS and EI_10FS.

As visible in Fig. 5a, for all samples analyzed, the low susceptibility of the modulus G' with respect to temperature indicates very good thermal behaviour in terms of elasticity. G'' turns out to be more susceptible, which means that temperature affects the viscous modulus more, and therefore the dissipation of the system. As visible in Figure 5 (a), the EI_10FS formulation has the highest moduli, both in terms of G' and G''.

It is important to note that as the fiber concentration increases, the gap between the moduli of the different concentrations decreases significantly, as can be seen in Fig. 5a, between EI_7.5FS and EI_10FS, suggesting a kind of limiting concentration, a saturation level, beyond which the fiber does not swell and therefore does not act any further because it has probably absorbed all the water in the system.

Looking at the phase angle (Figure 5 (b)) it is possible to note that for all the formulations there is an increase in the phase angle up to a certain temperature, probably due to a structuration of the fiber.

In this regard, it is important to give two important information about the fiber; first about the orientation and then about the microscopy. Usually, the fibers classically used in the literature are rod-shaped and therefore tend to be oriented in most cases. The fibers analyzed, on the other hand, are not oriented systems, since they are of different shapes, irregular, some

more elongated, others globular, thus random systems as it is possible to observe from Fig. 6. In Tab.7. is reported the Particle Size Distribution of the fiber used in this work.

Fig.6: SEM images of fiber, at 70x and 500x of magnification, utilised for fiber-addition emulsion.

Particle Size Distribution		
Dx (10) (µm)	**Dx (50) (µm)**	**Dx (90) (µm)**
35.5	124	318

Tab.7: Particle size distribution of fiber analyzed.

3.3.3 Recovered bitumen from fiber-added emulsion

Further rheological tests involved the bitumen recovered from the various emulsion-fiber formulations, shown in Fig.7, carried out on the base emulsion precisely to understand the fiber's single contribution to residual bitumen.

Fig.7: Recovered bitumen from fiber-added emulsions

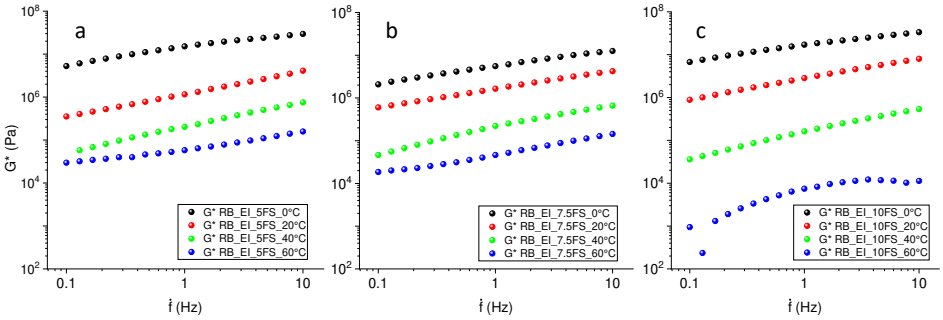

Fig.8: Overlay Frequency Sweep Tests of RB_ EI_5FS, RB_EI_7.5FS and RB_EI_10FS.

Fig.8 shows the results of the complex modulus of fiber-added recovered bitumen at various load frequencies and four temperatures. The results clearly show that is a typical viscoelastic material dependent on loading frequency and temperature. The behaviour is in agreement with the literature for emulsion with cement addition (Rutherford et al., 2014) the complex modulus increases with increasing frequency and decreases with increasing temperature.

Figure 8(a) depicts the behaviour of sample EI_5FS across the tested temperatures. The trend of the modulus appears favourable, maintaining a good response as frequency varies from high to low temperatures. This characteristic seems to improve further at 60°C, where the curve exhibits a lower slope, indicating a reduced dependence on frequency. This observation aligns with the findings in Figure 5, suggesting that the fiber likely undergoes a structuring process at higher temperatures, making it less susceptible to variations, potentially including frequency variations.

In fact, Fig.8 (b) and Fig.8 (c) show a pattern of modules very similar to the previous one, so the same considerations could be reported, simply with a smaller gap of difference of complex modules, particularly between T=0°C and T=20°C.

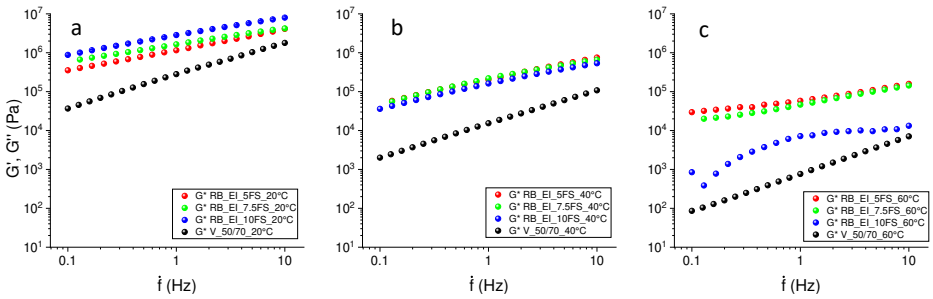

Fig.9: Overlay Frequency Sweep Tests of RB_ EI_5FS, RB_EI_7.5FS, RB_EI_10FS and V_50/70 at T=20°, 40° and 60°C.

Overlay of Frequency Sweep Test was realized at T=20°, Fig.9a, T=40°C, Fig.9b and T=60°C, Fig.9c. A marked improvement from all formulations with fiber compared to the base bitumen emulsion is evident. At T=20°C, depending on the formulation, the complex modulus increases by one/two orders of magnitude compared to virgin bitumen. Furthermore, the unfilled material (referring to the sample without fiber) exhibits a significant slope in its modulus, indicating a high sensitivity to frequency variations. This sensitivity is demonstrably reduced upon fiber addition, as discussed previously and evident in Figure 9a.

Fig.9b shows the same kind of improvement both in terms of modulus increase and frequency dependence, albeit on different values because the moduli are generally lower.

At 60°C, Fig. 9c reveals that the moduli of the fiber-reinforced emulsions remain two orders of magnitude higher than that of virgin bitumen. This advantage is coupled with a lower slope in the curves, signifying a weaker dependence on frequency variations. The only exception appears to be the RB_EI_10FS formulation, which exhibits a drop in modulus at this temperature. This observation might be attributed to an excess of fiber content.

These findings align with the viscosity improvements observed in Figure 3, where fiber addition yielded similar benefits in cementitious materials. However, it's important to note that compared to asphalt binders and mixtures, cementitious materials (CEA) inherently possess a higher complex modulus. This can be explained by the asphalt components being embedded and restricted within the cement paste matrix, leading to a more structured and consistent system (Tyler Rutherford et al., 2014).

Overall, this result is highly promising. As highlighted in the introduction, numerous materials have been explored for enhancing mechanical performance, but few achieve significant improvements at low inclusion levels. Xing Fang et al. investigated the impact of limestone filler content on the viscosity and complex modulus of bitumen emulsions (Fang et al., 2016). Their findings demonstrated that filler addition resulted in modest increases in both properties, but importantly, the blends exhibited minimal time-dependent viscosity changes over two hours.

Bibliography

Albayati, A., Wang, Y., Wang, Y., & Haynes, J. (2018). A sustainable pavement concrete using warm mix asphalt and hydrated lime treated recycled concrete aggregates. Sustainable Materials and Technologies, 18, e00081. https://doi.org/10.1016/J.SUSMAT.2018.E00081

Alkins, A. E., Lane, B., & Kazmierowski, T. (2008). Sustainable pavements environmental, economic, and social benefits of in situ pavement recycling. Transportation Research Record, 2012(2084), 100–103. https://doi.org/10.3141/2084-11

Borhan, M. N., Suja, F., Ismail, A., & Rahmat, R. A. O. K. (2007). Used cylinder oil modified cold-mix asphalt concrete. Journal of Applied Sciences, 7(22), 3485–3491. https://doi.org/10.3923/jas.2007.3485.3491

Boucard, L., Schmitt, V., Farcas, F., & Gaudefroy, V. (2015). Bitumen emulsions formulation and destabilisation process relationship: influence of salts addition. Road Materials and Pavement Design, 16(May), 330–348. https://doi.org/10.1080/14680629.2015.1030910

Cardone, F., Grilli, A., Bocci, M., & Graziani, A. (2015). Curing and temperature sensitivity of cement-bitumen treated materials. International Journal of Pavement Engineering, 16(10), 868–880. https://doi.org/10.1080/10298436.2014.966710

Chailleux, E., Ramond, G., Such, C., & De La Roche, C. (2006). A mathematical-based master-curve construction method applied to complex modulus of bituminous materials. Road Materials and Pavement Design, 7(November 2014), 75–92. https://doi.org/10.1080/14680629.2006.9690059

Dickinson, E. (2003). Hydrocolloids at interfaces and the influence on the properties of dispersed systems. Food Hydrocolloids, 17(1), 25–39. https://doi.org/https://doi.org/10.1016/S0268-005X(01)00120-5

Fang, X., Garcia-Hernandez, A., Winnefeld, F., & Lura, P. (2016). Influence of Cement on Rheology and Stability of Rosin Emulsified Anionic Bitumen Emulsion. Journal of Materials in Civil Engineering, 28(5), 1–12. https://doi.org/10.1061/(asce)mt.1943-5533.0001454

Garilli, E., Autelitano, F., & Giuliani, F. (2019a). Use of bending beam rheometer test for rheological analysis of asphalt emulsion-cement mastics in cold in-place recycling. Construction and Building Materials, 222, 484–492. https://doi.org/10.1016/j.conbuildmat.2019.06.141

Garilli, E., Autelitano, F., & Giuliani, F. (2019b). Use of bending beam rheometer test for rheological analysis of asphalt emulsion-cement mastics in cold in-place recycling. Construction and Building Materials, 222, 484–492. https://doi.org/10.1016/j.conbuildmat.2019.06.141

Goyer, S., Dauvergne, M., Wendling, L., Gaudefroy, V., Ropert, C., Envi, C. R., Laboratoire, O. /, De, R., Brieuc, S., & Dauvergne, F. M. (2012). Environmental data of cold mix using emulsified bitumen for a better selection of road materials. ISAP, France, 1–12. https://hal.archives-ouvertes.fr/hal-00845930

Graziani, A., Godenzoni, C., Cardone, F., & Bocci, M. (2016). Effect of curing on the physical and mechanical properties of cold-recycled bituminous mixtures. Materials and Design, 95, 358–369. https://doi.org/10.1016/j.matdes.2016.01.094

Huang, W., Zhang, X., Yin, Y., & Cai, S. (2018). A Numerical Implementation of the Three-Dimensional Viscoelastic Model for Asphalt Mastic. International Journal of Civil Engineering, 16(5), 543–551. https://doi.org/10.1007/s40999-017-0160-4

Kalpana, M., Ramesh, B., & Sai, J. (2020). Experimental investigation on the properties of bitumen added with industrial waste (cast iron). Materials Today: Proceedings, 22, 1192–1195. https://doi.org/10.1016/j.matpr.2019.12.119

Lei, L., Li, R., & Fuddin, A. (2020). Influence of maltodextrin retarder on the hydration kinetics and mechanical properties of Portland cement. Cement and Concrete Composites, 114(August), 103774. https://doi.org/10.1016/j.cemconcomp.2020.103774

Marek Iwański 2011.pdf. (n.d.).

Miljković, M., Radenberg, M., Fang, X., & Lura, P. (2017). Influence of emulsifier content on cement hydration and mechanical performance of bitumen emulsion mortar. Materials and Structures/Materiaux et Constructions, 50(3). https://doi.org/10.1617/s11527-017-1052-4

Raposeiras, A. C. (2013). Construc tion and Buildi ng Materia ls Test methods and influential factors for analysis of bonding between bituminous pavement layers. Construction and Building Materials, 43, 372–381. https://doi.org/10.1016/j.conbuildmat.2013.02.011

Rutherford, T., Wang, Z., Shu, X., Huang, B., & Clarke, D. (2014). Laboratory investigation into mechanical properties of cement emulsified asphalt mortar. Construction and Building Materials, 65, 76–83. https://doi.org/10.1016/j.conbuildmat.2014.04.113

Serfass, J. P., Gaudefroy, V., Beghin, A., Odie, L., Verhee, F., de la Roche, C., & Wendling, L. (2012). A detailed assessment of grave-emulsion combining trial section monitoring and laboratory testing. 5th Eurasphalt & Eurobitume Congress, 11p.

Shu, X., & Huang, B. (2008). Dynamic Modulus Prediction of HMA Mixtures Based on the Viscoelastic Micromechanical Model. Journal of Materials in Civil Engineering, 20(8), 530–538. https://doi.org/10.1061/(asce)0899-1561(2008)20:8(530)

Tan, Y., Ouyang, J., & Li, Y. (2014). Factors influencing rheological properties of fresh cement asphalt emulsion paste. Construction and Building Materials, 68, 611–617. https://doi.org/10.1016/j.conbuildmat.2014.07.020

Thanaya, I. N. A. (2003). IMPROVING THE PERFORMANCE EMULSION OF COLD BITUMINOUS (CBEMs) INCORPORATING WASTE The University of Leeds School of Civil Engineering. July.

Wang, F., Liu, Y., & Hu, S. (2013). Effect of early cement hydration on the chemical stability of asphalt emulsion. Construction and Building Materials, 42, 146–151. https://doi.org/10.1016/j.conbuildmat.2013.01.009

Wang, Z., & Sha, A. (2010). Micro hardness of interface between cement asphalt emulsion mastics and aggregates. Materials and Structures/Materiaux et Constructions, 43(4), 453–461. https://doi.org/10.1617/s11527-009-9502-2

Yin, Y., Huang, W., Lv, J., Ma, X., & Yan, J. (2018). Unified Construction of Dynamic Rheological Master Curve of Asphalts and Asphalt Mixtures. International Journal of Civil Engineering, 16(9), 1057–1067. https://doi.org/10.1007/s40999-017-0256-x

Conclusions

This PhD work involved the development of three key areas of study for cold recycling, particularly for bitumen emulsions.

In the first part, the formulation and laboratory production process of bitumen emulsion, prepared through a rotor-stator system, were studied, referencing the industrial emulsion supplied by the company. Then, a set of emulsifiers was examined, and interface analysis was carried out to identify an environmentally sustainable surfactant that could partially replace the industrial one. As verification and confirmation of the interfacial phase results, emulsions with the new surfactants were produced in the laboratory and analyzed rheologically. Both steady and dynamic rheological tests were carried out to verify whether they respected the bulk characteristics of the industrial one. The results that emerged from this first part, both in terms of correct laboratory reproduction of the emulsion and partial replacement of the surfactant, were very interesting. In the second part, the focus was the application of laser diffraction microscopy on bitumen emulsions. The emulsion was optimized in terms of emulsification rate, and then analyzed by laser diffraction the emulsions were prepared with the various surfactants, at different pHs and over time, to identify the best in terms of particle size distribution (PSD) and stability and an innovative technique was adopted for recovering residual bitumen from emulsion, studied rheologically and according to the standards adopted by Europe on the analysis of recovered bitumen. A greener formulation was found in which part of the surfactant was replaced with a green biopolymer and also the pH of the emulsion was increased, making it more sustainable. Finally, the most important stage in the application of this material was studied: the breaking emulsion, when it separates from the water and creates a film around the aggregates, acting as a binder. Several parameters intervene in breaking emulsion, including the materials employed to absorb the water, such as the cement usually used. In this work, an attempt was made to replace cement with a material that is equally sustainable, but capable of decreasing the moduli in terms of stiffness and increasing the elasticity of the system, providing flexibility to the pavement. A citrus fiber was used as a substitute for this process. The results obtained were interesting and promising. In particular, the residual bitumen obtained can sustain heavy loads, thus excellent bearing capacity, evidenced by high elastic moduli (G') and low dependence on frequency, but the great peculiarity of this fiber is that it also increases the viscous, dissipative modulus, G'', greatly increasing the flexibility, directly related to the dissipative capacity. The fiber added to the emulsion provided the residual

bitumen with important characteristics, such as bearing capacity and at the same time flexibility, predicting excellent performance on the final pavement. The challenge related to strength was achieved, prompting further research and developments. This approach promotes environmental sustainability, offers energy savings, and potentially reduces costs. This work can be useful to the road industry in designing new additives and preparations, sustainability and performance, applying a scientific rather than empirical approach based on the rheology and microstructure of such systems.